DAS Departamento de Automação e Sistemas
CTC Centro Tecnológico
UFSC Universidade Federal de Santa Catarina

Further development of a laser measurement system for machine tool testing

Relatório submetido à Universidade Federal de Santa Catarina

como requisito para a aprovação na disciplina

DAS 5511: Projeto de Fim de Curso

Ricardo Hoffmann

Florianópolis, Julho de 2014

Further development of a laser measurement system for machine tool testing

Ricardo Hoffmann

Esta monografia foi julgada no contexto da disciplina
DAS5511: Projeto de Fim de Curso
e aprovada na sua forma final pelo
Curso de Engenharia de Controle e Automação

Prof. *Marcelo Ricardo Stemmer*

_____
Assinatura do Orientador

Banca Examinadora:

Dipl.-Wirt.-Ing. Martin Peterek
Orientador na Empresa

Prof. Dr.-Ing. Marcelo Ricardo Stemmer
Orientador no Curso

A preencher
Avaliador

A preencher
A preencher
Debatedores

Acknowledgements

I would like to acknowledge Professor Dr.-Ing. Robert Schmitt, director of the Department of Production Metrology and Quality Management Laboratory of the Machine Tools and Production Engineering (WZL) RWTH Aachen, for the opportunity that was given to me, and Professor Dr.-Ing. Marcelo Ricardo Stemmer, coordinator from the Control and Automation Engineering graduation course from UFSC, for the cooperation agreement that made this opportunity possible. Professor Dr.-Ing. Ricardo Rabelo, a professor of the same graduation course, must be mentioned too, because the big support with all the bureaucracy and documents related to the internship.

I would like to acknowledge the support of my direct supervisor in the WZL, Dipl.-Wirt.-Ing. Martin Peterek, coordinator of the Macro and Coordinate Metrology group, that provided the necessary support for my project and always found time in his busy schedule to sane my doubts and give me some direction to follow. Also, thanks for giving me freedom to develop the work on my own.

I would like to thank all my colleagues from the department for the cooperation that helped me when it was necessary.

I would like to thank my family that gave me not only financial support, but stimulated me to do this project. I would like to thank all friends that I made during this long walk in Aachen that turned the day-to-day more funny and motivated me to work more properly. Not only the new friends, but the old ones that are always with me, showing up when it was least exected.

Last but not least, I would like to thank my girlfriend, Paullina, for all the love, kindness and support she has shown during the time it took me to finalize my project. Also thank her for understanding my staying longer than initially planned.

Through the support of everyone mentioned here it was possible to do my project and write this thesis.

Resumo

Este relatório visa explanar o trabalho realizado durante o estágio na cidade de Aachen na Alemanha no laboratório WZL da universidade RWTH Aachen, detentora de um dos melhores cursos de engenharia mecânica da Alemanha. Este estágio teve duração de 10 meses, entre setembro de 2013 e junho de 2014. O estágio foi caracterizado como projeto final de curso, que tem como sua função validar a disciplina obrigatória de mesmo nome para o curso de Engenharia de Controle e Automação da Universidade Federal de Santa Catarina.

O WZL der RWTH Aachen têm como uma de suas áreas de atuação o ramo de metrologia e qualidade do controle de fabricação. Existem muitos processos de fabricação metal mecânica analisados e estudados pelo laboratório, dentre eles o processo de fresamento e o teste do alinhamento da ferramenta de corte desse tipo de máquinas. São estudados vários métodos inovadores para tornar o teste alinhamento da ferramenta de corte mais rápido e eficiente, reduzindo custos.

Dentre esses métodos, foi proposto um novo método de teste do alinhamento da ferramenta de corte, englobando um sistema absoluto de medição a laser por interferometria existente no laboratório, conceitos de um sistema de medição desenvolvido no Linear Collider Alignment and Survey (LiCAS) e um sensor PSD (Position Sensitive Detector), capaz de medir a posição do laser.

Diante dessa proposta, foram realizados estudos no campo de interferometria para a concepção de um esquema que possibilitasse realizar as medições requisitadas envolvendo os conceitos anteriormente citados. Com a concepção de um esquema, foram pesquisados os componentes a serem comprados que satisfizessem os requisitos mínimos de desempenho.

Após a compra dos equipamentos, o sistema foi montado juntamente com os componentes já existentes. Porém, necessitou-se da elaboração de um processo de calibração para o sensor PSD, o que não foi previsto no primeiro cronograma e acabou causando um leve atraso. Foi desenvolvido um software na linguagem NI LABview para realizar a leitura do sensor PSD no computador e sua calibração.

Os dados da calibração tornaram possível ver em qual condição o sensor PSD desenvolvia melhor desempenho e pôde ser levado em conta para a montagem do esquema final.

A partir disso, métodos para a validação das medições realizadas pelo sistema desenvolvido foram desenvolvidos e analisados.

Abstract

This report aims to explain about the work done during the internship in Aachen, Germany at the Laboratory of the Machine Tools and Production Engineering (WZL) RWTH Aachen University, owner of one of the best mechanical engineering graduation course from Germany. This internship lasted 10 months, from September of 2013 to June of 2014. This internship was made for the final course project chair of the Control and Automation Engineering graduation course of the Federal University of Santa Catarina.

The Laboratory of the Machine Tools and Production Engineering (WZL) RWTH Aachen studies in one of his interest areas metrology and quality control manufacturing. There are a lot of metalworking manufacturing processes being studied and analyzed by the laboratory, the milling process and the test of the alignment of the cutting tool are among them. A lot of innovative methods for testing faster and more accurate the alignment of the cutting tool are being studied in order to reduce costs and improve quality.

Among these methods, it was proposed a new test method to check the alignment of the cutting tool using an existent absolute laser interferometry measurement system, concepts from a measurement system developed by the Linear Collider Alignment and Survey (LiCAS) and a PSD (Position Sensitive Detector) sensor, able to measure the laser position.

With this new proposal, studies were conducted in the field of interferometry to design a scheme that would allow performing the required measurements involving the concepts mentioned above. With a scheme developed, components that fulfilled the necessary performance requirements were searched to be purchased.

After the purchase of the equipment, the system was assembled together with the existing components. However, it was needed to prepare a calibration process for the PSD sensor, which was not specified in the first schedule and ended up causing a slight delay. A Software in LabVIEW language for reading the PSD sensor on the computer and calibration was developed.

Calibration data made it possible to see in what condition the PSD sensor developed better performance and could be taken into account when assembling the final scheme.

Afterwards, methods for validating the measurements performed by the developed system were developed and analyzed.

Summary

Table of figures

Chapter 1: Introduction

Machine tools and all kinds of measuring machines with three or more axes can be widely found in the industry at all areas of modern production. These machines can be found from automotive to aerospace industries, from production of consumer goods to medical goods. The trend toward individualized goods and minimize the lots sizes demands a huge flexibility of the machine tools. Following this concept, instead of relying on single purpose machines, production cells are built in order to improve this flexibility. The market of machine tools is growing and needs more performance from each machine separately.

The key to improve the performance for a modern production cell is to improve the ability to manufacture accurate parts. In order to achieve this accuracy of production, a controlled and deterministic manufacturing process is needed. The repeatability of the machine is necessary to control the process; while the geometric accuracy can be achieved by a feedback loop trough part metrology or using accurately calibrated machine tools to produce the parts.

In consequence of shorter product life cycles and small series production, the absolute accuracy of machine tools is really necessary and important.

Short-production ramp up times do not allow an iterative optimisation of the product quality. McKeown introduced the term volumetric accuracy to define the ability of a machine to produce accurate 3D shapes [2]*. Volumetric accuracy minimizes the ramp up cost for new or changing processes. Volumetric accuracy of machine tools and co-ordinate measuring machines (CMMs) has to be assured by precise and traceable metrology. The information gained may be used to characterize the machine or to increase the accuracy by numerical compensation.* [1]

To increase the absolute accuracy of the machine tools is really important to perform an error mapping and a subsequent compensation of geometric errors. For this purpose, it is extremely required an understanding of the sources and the effects of geometry errors in machines and calibration procedures.

Following this philosophy, every company wants to be really competitive in your work field. So the company needs to power the efficiency and quality to deliver a better product with lower price. This force the companies to improve the process quality to high standards. The companies need to get better in any small detail and save resources.

One of these details consists in checking the alignment of the cutting tool from a milling machine, which helps improvig the absolute accuracy of the machine. Providing a good test of the alignment of the cutting tool helps to deliver more accuracy to the operation, resulting in a higher quality product. Improving the speed of the alignment test helps to get this product faster, reducing its cost. Thinking this way is proposed here an innovative method for the testing process of the machine's alignment.

The results of this research can be used alone or maybe integrate with other existing test tool or research for the machine alignment.

The development of this test method is explained in the next chapters.

1.1: Company Overview: WZL

The Laboratory of the Machine Tools and Production Engineering (WZL) RWTH Aachen is placed at RWTH Aachen University. The laboratory is responsible for studies in these main fields:

- Metrology and Quality Management
- Production Engineering
- Manufacturing Technology
- Machine Tools

The WZL has about 830 employees. About 220 scientific staff coordinate and handle our research projects. They are supported by 190 non-academic staff and 420 student assistants.

The Laboratory is known worldwide for decades been synonymous with successful and pioneering research and innovation in the field of production technology. The Machine Tool Laboratory is managed by the four professors Christian Brecher, Fritz Klocke, Robert Schmitt and Günther Schuh. Figure 1 shows the main building of the WZL.

Figure 1 - WZL der RWTH

1.1.1: Macro and Coordinate Metrology Group

There are specific departments in the laboratory, this work takes place at the Macro and Coordinate Metrology Group department.

The integration of coordinate measuring technology in the manufacturing environment opens up extensive rationalization potentials. The work of the group focus in the holistic approach and continuous development of the CAx-based process chain from design and test planning to test data.

The group developed against these background solutions for all issues of process optimization and assist to obtain a continuous integration of this complex, high-performance measurement technology to the production environment.

1.2: Problem Presentation and Objectives

All the machine tools used to do metalwork processes are subjected to different forces and different temperatures during the operation, which after certain time causes some misalignment in the machine and can cause errors in the operation resulting in a product with low aggregate quality. This low quality product probably will have to be remade. So there is a waste of material and time, leading to

a waste of money, which should be avoided. In the next subsections it will be presented the source of these errors.

1.2.1: Alignment Errors Source

The accuracy of machine tools and CMMs is affected by many error sources. These error sources may cause a change in the geometry of the machine's components present in the machine's structural loop. According to ANSI and ASME standards [3] *a structural loop is defined as an assembly of mechanical components which maintain a relative position between specified objects. In a machine tool, the structural loop includes the spindle shaft, the bearings, the housing, the guideways and frame, the drives and the tool and work-holding fixtures. Due to a change in geometry of these structural loop components, the actual endeffector position and orientation relative to the workpiece differs from its nominal position and orientation, resulting in a relative orientation and positioning error. The magnitude of this positioning and orientation error depends on the sensitivity of the machine's structural loop on various error sources.*

The following reported major error sources affect the accuracy of the relative end-effector position and orientation [4] [5] [6]*:*

- *Kinematic errors;*
- *Thermo-mechanical errors;*
- *Loads;*
- *Dynamic forces;*
- *Motion control and control software.*

In precision instruments and machines many parts interact to achieve a final accuracy. Each part contributes to the total accuracy due to deviations caused by the above-mentioned effects. Although in practice the interaction between these effects plays an important role in the overall system behaviour, here we will focus on these effects separately. [1]

1.2.1.1: Kinematic Errors

Kinematic errors are errors due to imperfect geometry and dimensions of machine components as well as their configuration in the machine's structural loop, axis misalignment and errors of the machine's measuring systems [7] [8] [9]*. If*

the position of one axis influences the location and component errors of another, then the single errors of this axis are functions of the axis under test and of the influencing axis. Furthermore location errors might also become functions of axis positions. In principle, the systematic of kinematic errors stays the same, but the error functions become more complicated. [1]

1.2.1.2: Thermo-mechanical Errors

Due to the presence of, sometimes changing, internal and external heat/cold sources in machine tools and CMMs and the very often significant expansion coefficients and expansion coefficient differences of machine part materials, the resulting thermal distortion of the machine's structural loop often dominate the accuracy of an executed task [10] [11]*. Expansion coefficient differences may lead to thermal stresses if rules of exact constraint design have not been met carefully. Changed thermal conditions may cause location and component errors of machines.* [1]

1.2.1.3: Loads

If a machine exhibits non-rigid body behaviour, location erros and component errors change due to internal or external forces [12]*. In some cases, the weight and position of for instance the workpiece or moving carriages of the machine, or the static machining—or measuring forces can have a significant influence on the machine's accuracy due to the finite stiffness of the structural loop. Schellekens et al.* [12] *and Spaan* [5] *have shown that these errors can be significant when compared to the kinematic errors of a machine tool or CMM. For instance, if straight guideways bend due to the weight of the moving slide, the slide will show a vertical straightness and a pitch error motion. This is called "quasi-rigid behaviour". Such effects will be caught by measuring the error motions and do not change the systematic of the error description.* [1]

1.2.1.4: Dynamic Forces

The trajectory to be realized by a machine tool or a CMM is also affected by the dynamic behavior of the machine's structural loop. In this case (rapidly) varying forces such as machining forces, measuring forces or forces caused by accelerations

or decelerations should be considered instead of quasi-static ones. Vibrations may result in a deformation of the structural loop of the machine under consideration. The deformations due to vibrations in the structural loop are often hard to compensate. This is due to the very often unknown amplitude and in particular the phase angle of the vibration frequencies. This contributes to the uncertainty of the tool/probe position relative to the workpiece. Relevant information concerning deviations due to dynamic forces can be found in [6] [13]*.*

Motion control and control software effects on the geometrical error can be significant. In the analysis, they are often distinguishable from the errors caused by other error sources by applying different feed speeds and/or accelerations for the same motion path.

However, precision machining or measuring is often carried out at small feed speeds, with small acceleration and decelerations as well as small cutting/measurement forces. Error correction and compensation, without taking these dynamic forces into account, can, nevertheless, be successful in these cases. [1]

Figure 2 - Hermle Milling Machine

Figure 2 shows an example of the machine tool that is the subject of this study.

1.2.2: Project Objectives

To avoid problems due to these errors in the final product, a test of the alignment of the cutting tool must be done, among some operations to check if the alignment remains acceptable. There are some conventional technics to do this alignment test, like using a complex and expensive machine, which can be very accurate but takes a long time and effort. So the subject of this research is to develop an innovative alignment test method with new technologies based on laser techniques that aim to be easy and faster than traditional methods. It is expected to use some of the powerful capabilities of the laser measurement system owned and sensors to measure laser position too.

This project has the following main steps:

- Research and study of laser measurement techniques;
- Search and buy hardware that could fit the specifications;
- Software development
- Calibration of the sensors;
- Built of the system;
- Validation.

This work has the general objective of:

- Research and development of a faster and more efficient method of testing the alignment of machine tool;

And there are some specific objectives:

- Make use of the laser measurement system owned;
- Create knowledge for further projects;
- Create an accurate and reliable system;
- Create a knowledge base of sensors to read laser position.

1.3: Document Structure

This work is divided into seven chapters. The first one gives a brief introduction about the company, describes the context of the project and provides its motivations and objectives.

The second chapter presents a bibliographical revision of the concepts of interferometry, how a PSD (Position Sensitive Detector) sensor works and the Linear Collider Alignment and Survey (LiCAS) concept, which the system was based.

The third chapter explains the concept that was developed to create the measurement system and presents the mathematical background of this concept too.

The fourth chapter presents all the components used in the system divided into two categories, hardware and software.

The fifth chapter shows how the calibration of the PSD (Position Sensitive Detector) was performed. In this chapter it is presented the system mounted and the design of a platform for the whole system. Further, some techniques to validate the system are presented.

The sixth chapter presents the results obtained: the calibration of the PSD sensor and the results of the validation tests for the project.

The seventh and last chapter shows the conclusions obtained during the realization of the project, and it leaves, as well, suggestions for future improvements in the system.

Chapter 2: Theoretical Background

This chapter presents theoretical information about the main physics concepts that are the background for the project.

2.1: Introduction to Interferometry

The phenomenon of interference occurs when two light waves are superposed, and the result of the intensity at any point depends on whether they increase or decrease each other. When two waves with the same frequency combine, the resulting pattern is determined by the phase difference between the two waves. Therefore, the waves that are in phase will be subjected to constructive interference as well as the waves that are out of phase will go through destructive interference. This phenomenon can be observed in Figure 14:

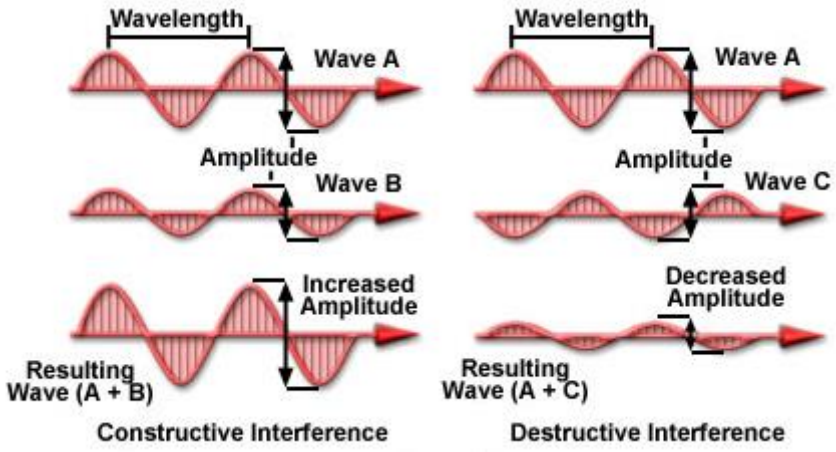

Figure 3 - Interference between coincident Light waves [14]

The wavelength of visible light is very small and a few alterations in the optical path difference create measurable changes in the intensity of an interference pattern. For this reason the optical interferometry allows highly accurate measurements.

With the basic principle of using a very small, stable and accurately defined wavelength of light as a unit of measure, interferometry acquires substantial information using the phenomenon of interference applied in many electromagnetic waves.

Optical interferometry has been applied as a laboratory technique since the last century, and various advanced developments and research have increased its scope and accuracy, which made the optical interferometry benefits functional for an ample range of measurements. More details about interferometry can be found in [14].

2.1.1: Two-Beam Interferometers

To get measurements utilizing interference, it is essential to acquire an optical arrangement where two beams must interfere after they have followed separate paths. One path is called the reference path, while the other is the measurement path. Then, the optical path difference between the interfering wavefronts is:

$$\Delta p = p1 - p2 = \sum(n1*d1) - \sum(n2*d2)$$

Where "*n"* is the refractive index, and "*d"* the length, of each section in the two paths.

In order to produce a stationary interference pattern, it is important that the phase difference between the two interfering waves do not change with time. Thus, the two interfering beams must have the same frequency, which means they have to derive from the same source.

Wavefront division and amplitude division are the two methods generally used to divide the beam in two parts from a single source. Wavefront division uses apertures to isolate two beams from separate portions of the primary wavefront, while in amplitude division, two beams are derived from the same portion of the original wavefront using some optical elements. Figure 4 shows the interference of two beams formed by wavefront division:

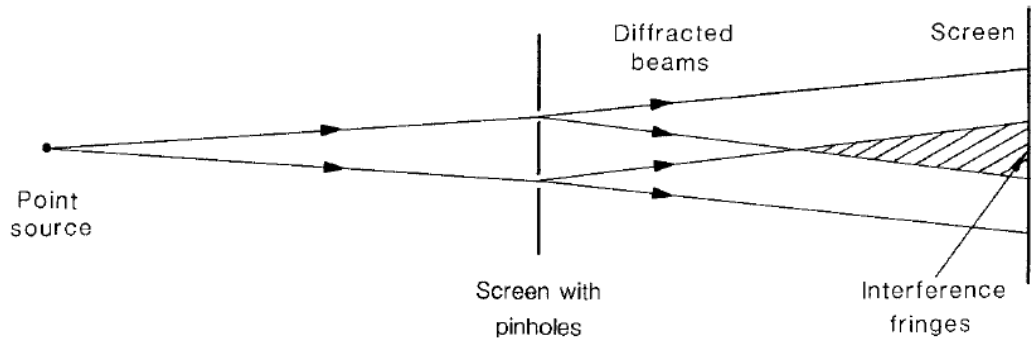

Figure 4 - Interference of two beams formed by wavefront division. [14]

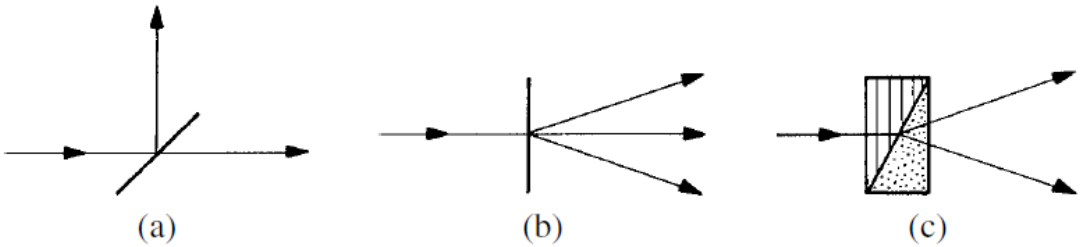

Figure 5 - Techniques for amplitude division: (a) a beam splitter, (b) a diffraction grating, and (c) a polarizing prism. [14]

Figure 5 shows techniques for amplitude division.

Some types of interferometers and their applications are:

• The Rayleigh interferometer - gas analysis;

• The Michelson/Twyman–Green interferometer – measurements of length and optical testing;

• The Mach–Zehnder interferometer - fluid flow, heat transfer, and the temperature distribution in plasmas;

• The Sagnac interferometer - rotation sensing. [14]

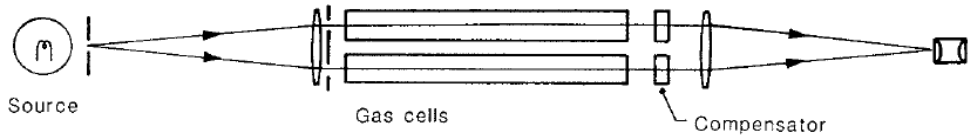

Figure 6 - The Rayleigh interferometer. [14]

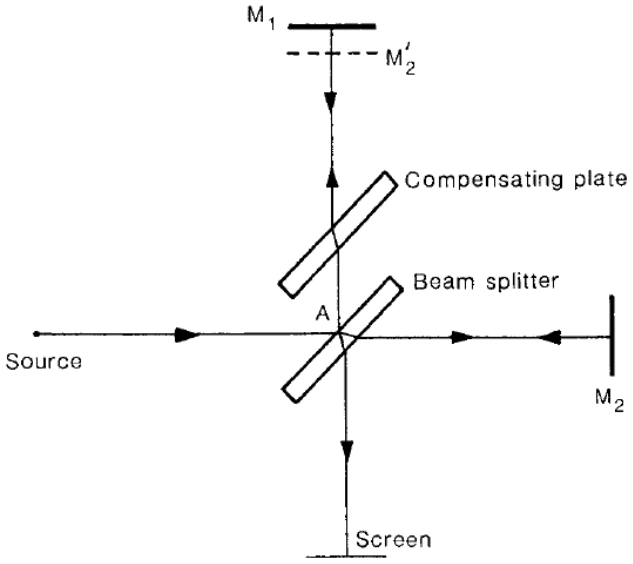

Figure 7 - The Michelson interferometer. [14]

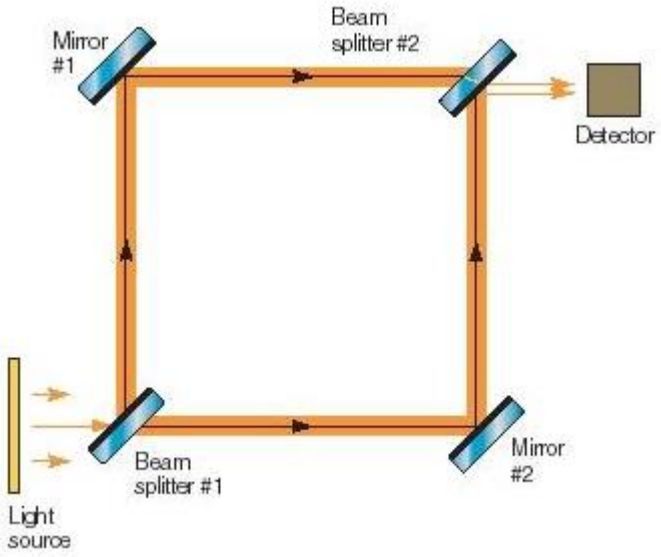

Figure 8 - The Mach–Zehnder interferometer [14]

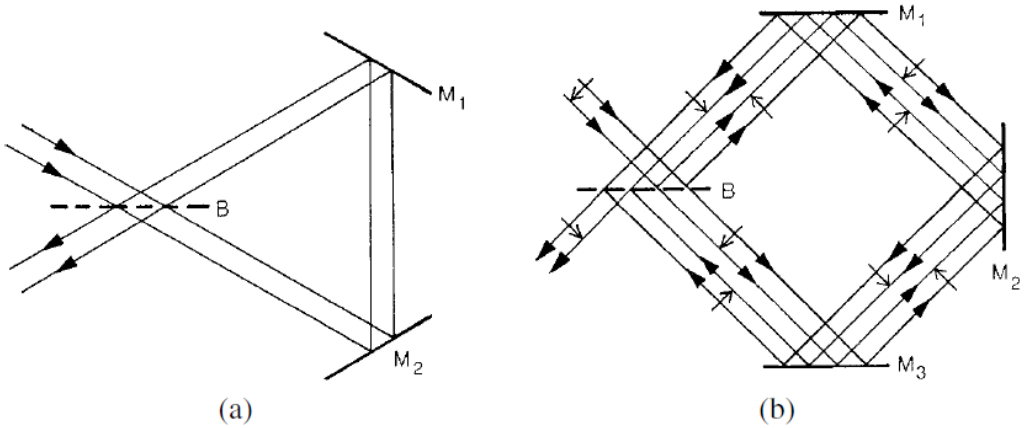

Figure 9 - Two forms of the Sagnac interferometer: one with an even number of reflections in each path (a), and the other with an odd number of reflections in each path (b). [14]

2.1.2: Laser Interferometers

An interferometer is a very precise instrument that measures distances with high accuracy. The idea of a laser interferometer is to use the principle of interferometry to retrieve the information of the destructive and constructive superposition of the electromagnetic waves during the data acquisition.

It works taking a laser beam and dividing it into two parts using a beam splitter: one of the beams (which is the reference beam) travels to a reflector and from there

to a detector, while the other beam travels through the distance that is being measured, pass onto a second reflector and goes back through the beam splitter, and onto the same detector as the first beam. Since the second beam travels a different distance to the first beam, it gets out of phase. The two beams reunite at the detector and interfere, thus the phase difference between them creates an interference fringes/pattern. Therefore, by observing and measuring the fringes, it is possible to calculate accurately this distance. Figure 10 shows an Interferometer example.

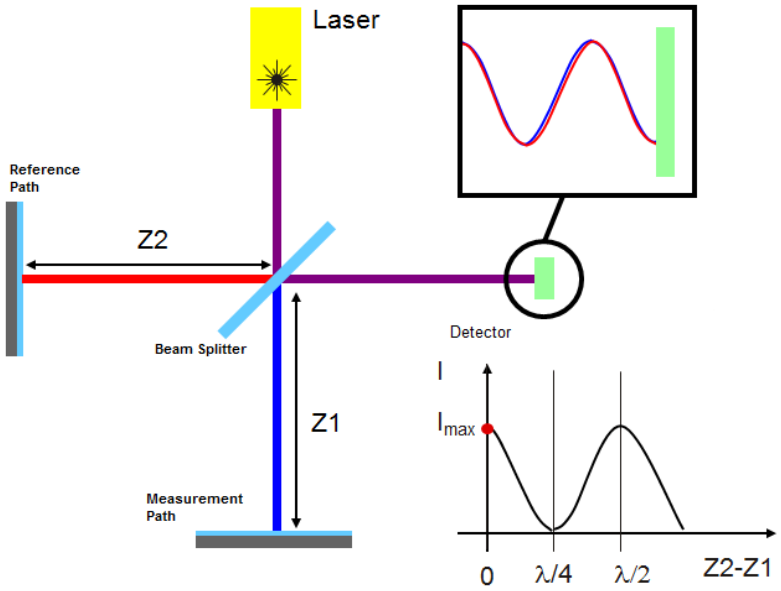

Figure 10 - Interferometer example [14]

In laser interferometric systems, in which distances are measured precisely, the wavelength of the utilized laser light in a medium must be cognized with high accuracy. The wavelength is determined by the vacuum frequency of the used light, the speed of light in the vacuum and the refractive index of the medium. Commonly the vacuum frequency of laser light has an uncertainty around 10^{-8} and 10^{-9}, while the speed of light in vacuum is constant. The predominant uncertainty component derives, therefore, from the uncertainty of the refractive index of air.

2.1.3: Frequency Scanning Interferometry

This is the measurement method used by the Multiline System used in the project, and follows the explanation:

In the simplest FSI system, a single tunable laser is used to compare interferometers with unknown optical path differences (OPD) to a common reference interferometer. Each interferometer is assumed to be an amplitude-splitting, two-arm interferometer.

The frequency of the laser is scanned continuously in one direction, to induce continuous, unidirectional phase changes in the reference interferometer and in all measured interferometers of unknown OPD. Each unknown interferometer is measured by comparing the phase change in its signal with the corresponding phase change in the signal from the reference interferometer.

In the following discussion, separate notation is used for the reference interferometer and the measured interferometers. The phase of the reference interferometer, with optical path difference (OPD) "$\mathcal{L}$" illuminated by a single laser of frequency "ν", is given by:

$$\Phi = \left(\frac{2\pi}{c}\right)\mathcal{L}\nu$$

Similarly, the phase of a measured interferometer with OPD "$\mathcal{D}$" is given by:

$$\Phi = \left(\frac{2\pi}{c}\right)\mathcal{D}\nu$$

As the laser is tuned through a frequency interval "$\Delta\nu$", the induced phase change in each interferometer ("$\Delta\phi$" or "$\Delta\Theta$") is therefore proportional to the OPD ("$\mathcal{L}$" or "$\mathcal{D}$" respectively). The interferometer phase ratio, q, is defined as:

$$q = \frac{\Delta\phi}{\Delta\Theta}$$

In the absence of OPD drift, this phase ratio q is equal to the ratio "$\mathcal{L}/\mathcal{D}$". The basic aim in an FSI measurement is to find "q" for each interferometer, so that the interferometer OPD can be determined using:

$$\mathcal{D} = \frac{\mathcal{L}}{q}$$

If there is OPD drift during the frequency scan, the OPD derived using equation "$\mathcal{D} = \mathcal{L} / q$ " with the phase ratio "q", measured using a single laser, would be

in error. A second laser is required to enable an appropriate correction to be applied. [15]

2.2: Introduction to Position Sensitive Detector (PSD)

The PSD sensors are used in the system because of the wavelength of the measurement laser, which is not visible causing no possibilities to use CCD cameras.

The Position Sensitive Detector (PSD) is a sensor, basically made of diodes, that tracks the laser and returns the position in the sensor range. The sensor can be one dimension or two dimensions. In this study is used a two dimensions PSD, so is this one will be presented.

There are two main PSD types: lateral effect and segmented detector. The quadrant detector, from the segmented family, was chosen because is more accurate and there were more possible options for the laser wavelength used.

The quadrant detector (QD) is a position detector based on the photovoltaic effect to determine the relative position of the light spot projected on its surface. It is made of four identical p–n junction photodiodes and the photodiodes are separated by small gaps called the dead area. Compared to other position sensitive detectors such as the lateral effect PSD and the charged coupled device, QD has the advantage of fast response frequency, wide response wavelength, high response sensitivity and wide operating temperature range. Due to these advantages, QD has been widely used to measure the beam displacement. Recently, the QD is becoming more and more important in the area of nanotechnology. However, when QD is used for high-precision measurements, some factors will influence QD measurement accuracy, dynamic range and sensitivity. The non-linear relationship between the light spot position and its estimate is reported in some literatures. The spot movement mode, spot energy distribution, and dead area will influence the dynamic range and the detection sensitivity. Thus, these factors analysis is highly desirable to improve the measurement accuracy of QD and enhance QD applications. [16]

2.2.1: Theoretical Model of the PSD

QD consists of four junctions placed symmetrically with respect to the center shown in Fig. 1. The photocurrents will be generated when a light beam is projected. The conventional formulas to estimate the beam position are expressed as follows:

$$X = k * \frac{Ia + Id - Ib - Ic}{Ia + Ib + Ic + Id}$$

$$Y = k * \frac{Ia + Ib - Ic - Id}{Ia + Ib + Ic + Id}$$

Where "X" and "Y" are the estimate of the beam position in the x and y directions, k is the slope constant whose value is dependent on the beam profile, and "Ia", "Ib", "Ic", and "Id" are the photocurrents measured at each quadrant. [16]

Figure 11 shows a schematic diagram for an example of quadrant detector:

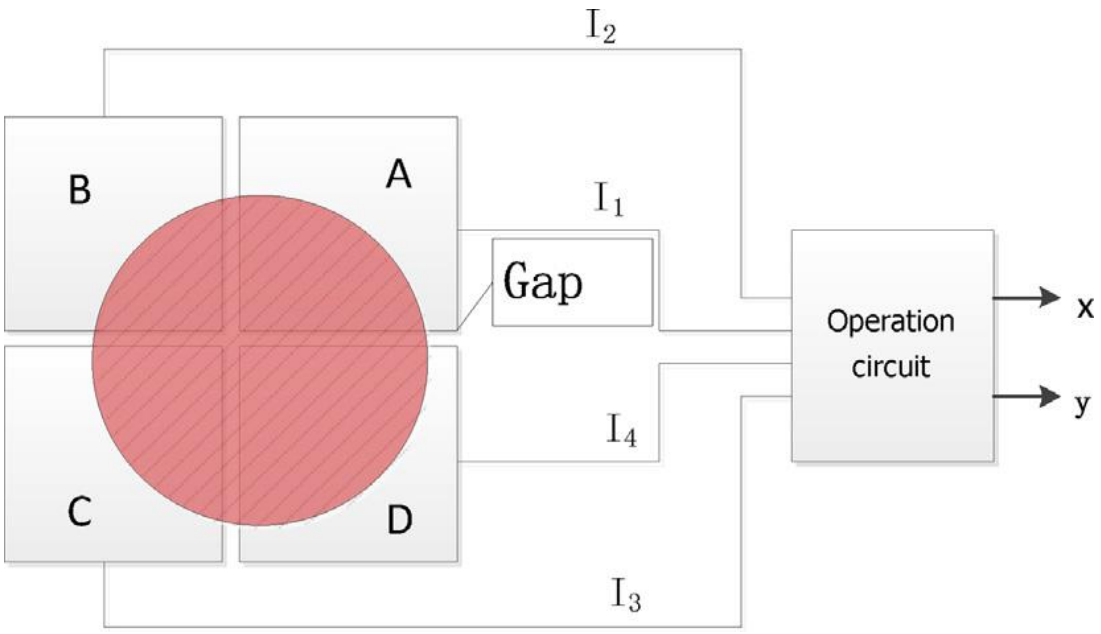

Figure 11 - Schematic diagram of the quadrant detector [16]

2.3: Introduction to the Linear Collider Alignment and Survey (LiCAS) Concept

The Linear Collider Alignment and Survey (LiCAS) group aims to provide an optical metrology system for the survey and alignment of a Linear Collider. It uses a combination of Frequency Scanning Interferometry (FSI) and Laser Straightness Monitors (SM) inside a vacuum. Both techniques have their origin in particle physics

detector alignment and have been developed at the University of Oxford. FSI is an interferometric length measurement system which was originally developed for the online alignment of the ATLAS Inner Detector. The SM is used in the alignment system of the Zeus MicroVertex Detector. [17]

The Laser Straightness Monitors (SM) allow the LiCAS survey train to measure inter-car transverse displacements and rotations. The technology has been used in the alignment system of the Zeus MicroVertex detector (MVD) which was developed at the University of Oxford.

In the survey train a collimated fibre coupled laser is used which has low longitudinal coherence length (50μm) but high transverse coherence. This allows efficient coupling into a single-mode optical fibre but reduces interference from spurious reflections. The beam is intercepted by a beam-splitter and the reflected beam goes to a CCD camera. The beam passes through six beam splitters in total; one beam-splitter per car. At the last car, the beam is reflected back via a retroreflector. The beam subsequently passes through the same beam splitters; thus each beam-splitter is intercepted twice. A second camera on the car observes the reflection off the second interception. This arrangement is illustrated in Figure 12. By correlating the images from the two cameras one can differentiate translations from rotations.

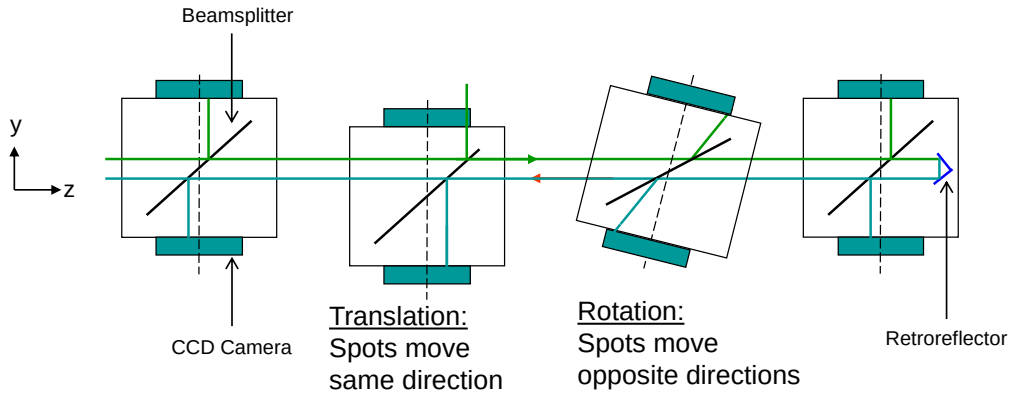

Figure 12 - Optical arrangement of SM in the LiCAS Survey Train: It shows one car which has been translated and one which has been rotated. It shows that for a translation, both beams on the CCD cameras move in concert. However for a rotation, the beams on the CCD move in contrary. [18]

In the Zeus MVD, the length of the SM is 2 m. For LiCAS the range of the SM must be twice the length of the train which is 50 m. To have a beam with minimal divergence requires a wide beam diameter to be greater than the CCD viewing area. This is compensated for by adding demagnification optics in front of the CCD cameras. The LiCAS SM uses two parallel beams to allow measurements of rotation about the z-axis [1]. This is illustrated in Figure 13. As the car rotates about the z axis, one observes the angle of the beams with respect to the CCD changes. The use of the single beam-splitter and retroreflector is one possible configuration for a SM. Another possible arrangement is to use two beam splitters at right-angles to each other. This avoids the need for a retroreflector. Both arrangements are currently under evaluation. [18]

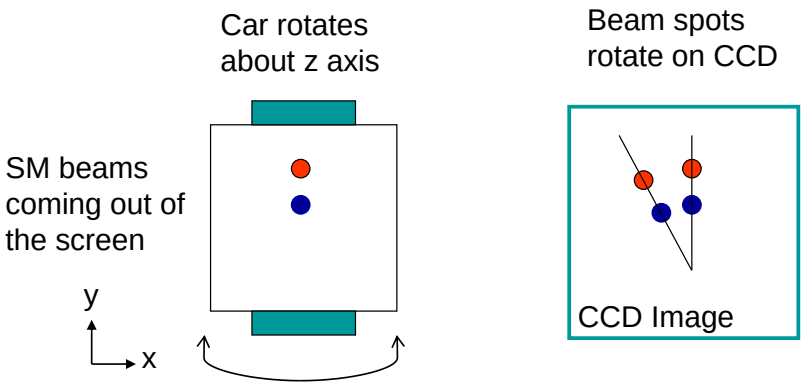

Figure 13 - Two SM beams allow rotation about the z axis to be measured: As the car rotates, the angle of the beams with respect to the CCD changes [18]

The LiCAS uses CCD image cameras to read out the laser position, before in this document was explained why this project uses Position Sensitive Detector (PSD) to read out the laser position and not CCD image cameras.

Chapter 3: The Laser Measurement System Concept

This chapter explains about the concept developed to create the laser measurement system and its capabilities. It also gives an analysis of the mathematical background.

3.1: The Concept developed for the Laser Measurement System

The proposed system should be able to perform measurements in length, rotation and lateral displacement. The system should be as more accurate as possible, taking into account the cost-benefit. Based on the LiCAS concept it was developed an idea of how to create this measurement system.

3.1.1: Schematic Diagram of the Laser Measurement System

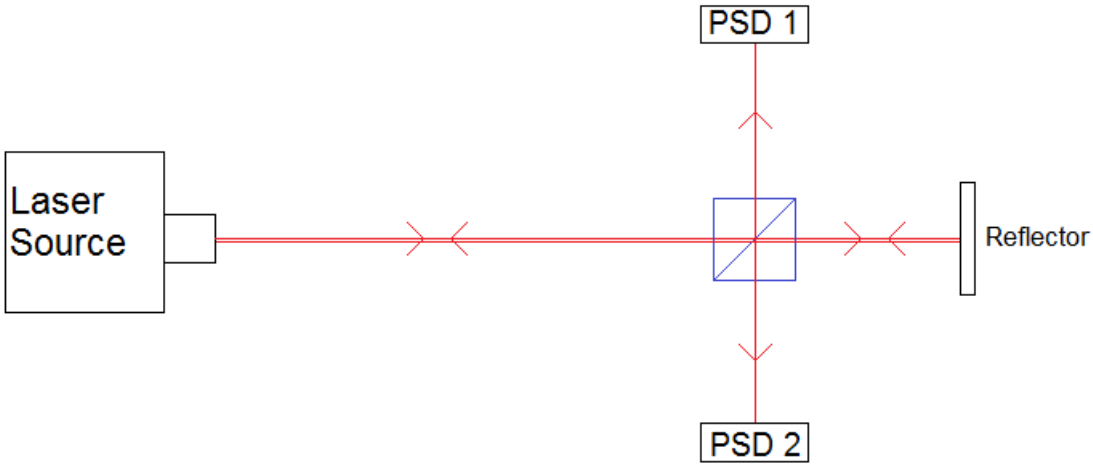

Figure 14 - Schematic diagram of the measurement system concept

The system will be mounted on a platform composed by the PSD 1, PSD 2, beamsplitter and retroreflector. The laser source will remain disconnected from the whole system. Figure 14 shows the main schematic diagram or the measurement system concept.

3.1.1.1: Components of the System

The system is composed by the following components:

- Laser Source: it is the laser that comes from the laser interferometry measurement system.
- Beamsplitter: it is a glass cube with a plate inside that splits the laser in two separated perpendicular beams.
- PSD 1 and PSD 2: these are the Position sensitive detectors to read out the laser position.
- Retroreflector: this is hollow retroreflector that reflects the laser beam back.

More technical details about the system components are presented in the chapter 4.

3.1.1.2: Trajectory of the Laser Beam

The laser beam starts its path in the laser source and then it goes to the beamsplitter that splits the laser beam into two beams: one goes to the PSD 1 and the other one goes through the beamsplitter. The one that goes through the beamsplitter hits the retroreflector and comes back to the beamsplitter. The laser beam splits again and the opposite happens: one beam goes to the PSD 2 and the other beam goes through the beamsplitter and hits the laser source. This last beam is used by the laser interferometry measurement system. The first split is shown in Figure 15 and both, first and second, are shown in Figure 16:

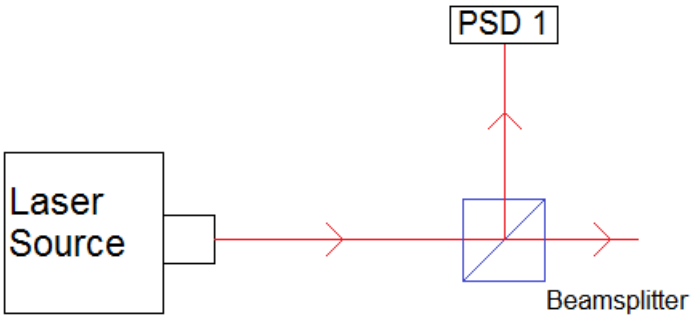

Figure 15 - First split in the beamsplitter

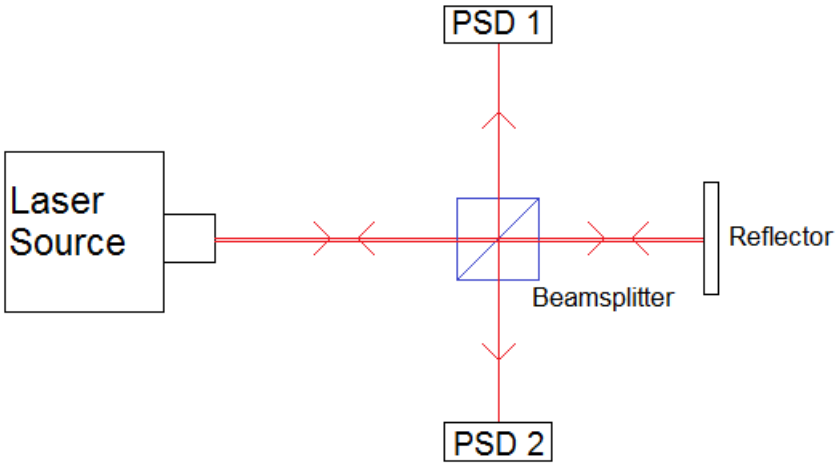

Figure 16 - First and second laser beam split together

3.1.1.3: Laser Energy Division

The laser splits its energy in the path when the laser beam splits. The beamsplitter has the characteristic of 50%/50% energy splitting in both ways. Considering that the initial energy from the laser source is 100% and an ideal situation, the first splits sends 50% of the energy to the PSD 1 and the remaining 50% of the energy to the retroreflector. The reflector reflects this 50% energy back and the beamsplitter splits it again: 25% to the PSD 2 and 25% is sent back to the laser source. Figure 17 helps to understand the energy splitting.

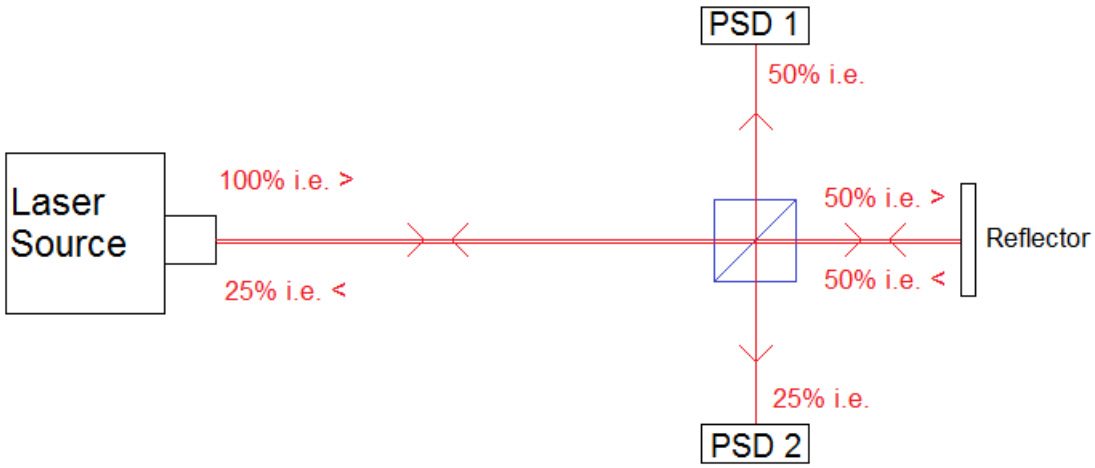

Figure 17 - Diagram of the energy splitting (i.e. means initial energy).

In Figure 17, the arrows near the percent values in the image are only used for demonstrating the direction of the laser.

3.1.2: Variables Measured

There are 3 kinds of displacement that are measured by the system:

- **Length measurement:** it is performed by the laser interferometry measurement system, and it uses the laser that comes back from the Beamsplitter. It reads the distance between the laser source and the retroreflector. The whole system (except the laser source) can move parallel to the laser source. This is shown in Figure 18 and the black arrows sign the movement direction.
- **Rotation measurement:** the rotation of whole system (except the laser source) can be measured by reading the outputs from the PSDs that change when the system rotates. This is shown in Figure 19 and the black arrows sign the movement direction.
- **Lateral displacement measurement:** the whole system (except the laser source) moves perpendicularly to the laser source. This displacement changes where the laser hits the beamsplitter, so it changes where it hits the PSD too. This change can be read out to calculate the lateral displacement, which is shown in Figure 20 (black arrows sign the movement direction).

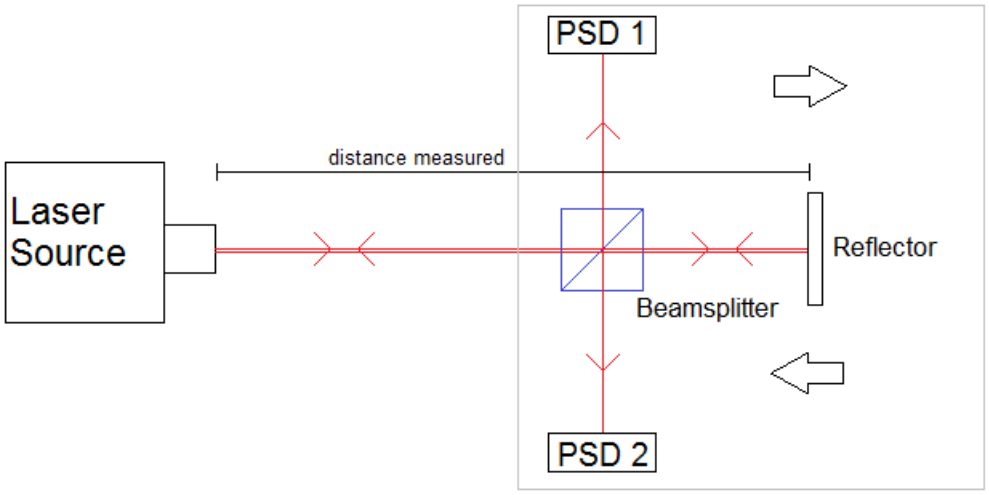

Figure 18 - Length measurement

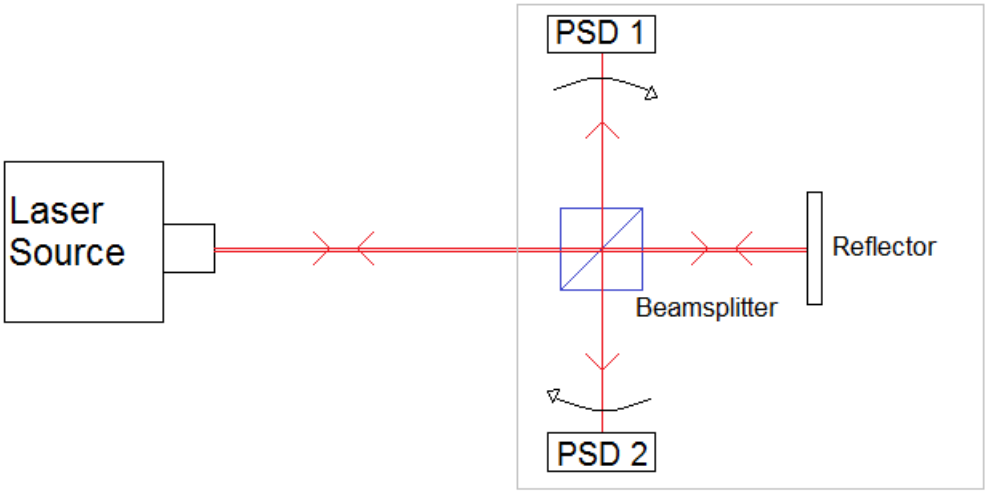

Figure 19 - Rotation movement

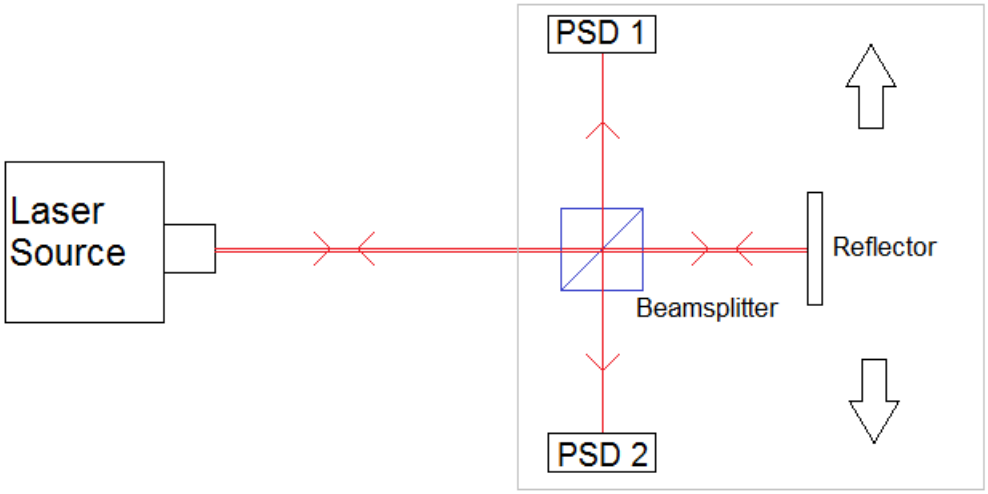

Figure 20 - Lateral displacement

3.2: Mathematical Background

This section aims to show the mathematical calculations that are done in order to get the measurement results. In the end, there is an error propagation analysis for the rotation measurement calculation.

3.2.1: Length Measurement

This measurement is performed by the interferometry laser system owned by the laboratory. The mathematical explanation about this measurement follows the idea given in chapter two (section 2.1.2). The only different thing about this measurement in a comparison with a normal measurement is that there is the glass cube in the beam's path and the laser loses more energy than normally expected. These effects will be presented in the results chapter.

3.2.2: Rotation Measurement

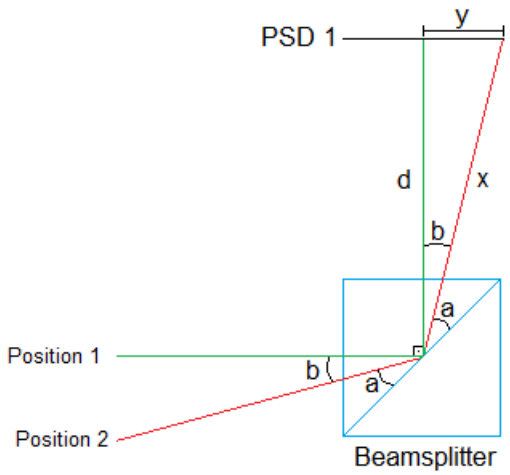

Figure 21 - Rotation measurement schema

The schema in Figure 21 presents two different positions for the same laser beam in different times. The goal is to know the rotation, in the schema the "b" angle. The distance "d" is fixed and it is from the center of the beamsplitter to the center of the PSD 1. The "Position 1" is the setup position and "Position 2" is a possible measurement position. The "y" value can be known by reading PSD 1 data output. Trigonometric laws allow saying that:

$$\tan b = \frac{y}{d}$$

$$\tan^{-1} b = \frac{y}{d}$$

The second equation returns as a result the “b” angle. A calculation with the width of the PSD 1 measurement range returns the maximal angle that can be measured.

This calculation does not take account of the diffraction and refraction that can occur when the incidence angle of the laser is different from zero degree. Considering small rotation angles this error can be ignored for now.

3.2.3: Lateral Displacement Measurement

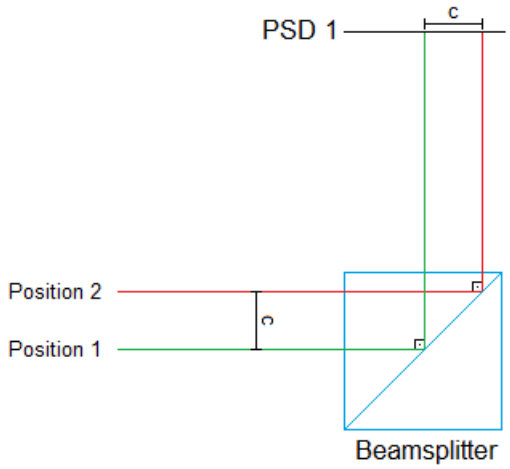

Figure 22 - Lateral displacement schema

The schema in Figure 22 presents two different positions for the same laser beam in different times. The goal is to know the lateral displacement, in the schema the “c” distances. The “Position 1” and “Position 2” are two possible measurement positions. The “c” value can be known by reading PSD 1 data output. Trigonometric laws allow saying that the distance “c” in the PSD 1 is the same distance “c” between “Position 1” and “Position 2”.

3.2.4: Error Propagation Calculation

Considering the rotation measurement, it is needed to know the distance from the center of the beamsplitter to the PSD sensor (“d” in Figure 21). This

measurement is exposed to some error because must be performed manually. There are others difficulties to perform this measurement like the PSD sensor is not on the surface of the mounting case and is not so easy to see where the middle of the beamsplitter is. These difficulties can be solved, but still it can cause some error in the measurement.

On this purpose an error propagation analysis was performed to see the influence of this measurement error in the final result.

The variable that must be analyzed is "d", the distance in the PSD is "p" ("y" in Figure 21) and "φ" is the angle.

$$\varphi = \tan^{-1}\left(\frac{p}{d}\right)$$

Error propagation:

$$\sigma_\varphi = \sqrt{\left(\frac{\partial\varphi}{\partial p}\right)^2 \sigma_p^2 + \left(\frac{\partial\varphi}{\partial d}\right)^2 \sigma_d^2} = \frac{1}{1+\frac{p^2}{d^2}} * \frac{1}{d}\sqrt{\sigma_p^2 + \frac{p^2}{d^2}\sigma_d^2}$$

It can be seen that error in "p" dominates as long as the relative error of "d" is small.

Chapter 4: Hardware and Software System Components

This chapter presents technical information about the hardware and software used in the project. The technical details were taken from the product datasheet.

4.1: The Absolute Multiline System

The Absolute Multiline system is an absolute measuring interferometer to measure and control lengths between 0,2 to 20 meters within 24 channels. The system is expandable to 50 channels. The patented “Snapshot Phase Shifting Interferometry” realizes a precision of the length measurement of 0,5 µm +0,5µm/m. The system needs a short time to determine a length. This measuring time decreases with shorter distances. The measurement is done with two frequency-scanned lasers. A gas cell assures traceability of their frequencies. For more information consult the datasheet in [19].

Figure 23 - The Multiline measurement system by Etalon

4.1.1: Measurement Line

Method: direct, absolute length measuring system

Accuracy of displacements: 0.5 µm + 0.5 µm/m

Wavelength: Pilot 635 nm (alignment laser) / Measuring 1410-1510 nm

Laser class: 2

Reflectors: 24 hollow retroflector

Collimators: 24 FC-collimators with fine adjustment knobs

Environment: USB humidity and pressure sensor

Interface: USB-2

4.1.2: Working Range

Measurement range: 0,2m – 20m

Channels: 24

Max. Frequency: 100 kHz per snapshot

Snapshots: 2 /s

4.1.3: Environmental Conditions

Temperature range for accuracy specification: 15 °C to 35 °C

Humidity: 0% to 80% non-condensing

4.1.4: Additional Tools

Etalon provides with the Multiline laser measurement system tools for aligning the laser and adjusting it and the reflectors. The hollow reflector can be seen in Figure 24. The mount and adjust tools for the laser collimators can be seen in Figure 25.

Hollow Retroreflectors are constructed of three first surface mirrors assembled into a corner cube. This produces a lightweight “hollow corner cube” that is totally insensitive to position and movement. The result is that parallel incident light is reflected back to the source with great accuracy, regardless of the angle of incidence.

Since the optical path is in air, this configuration eliminates material absorption and chromatic aberrations present in solid glass prism-type retroreflectors.

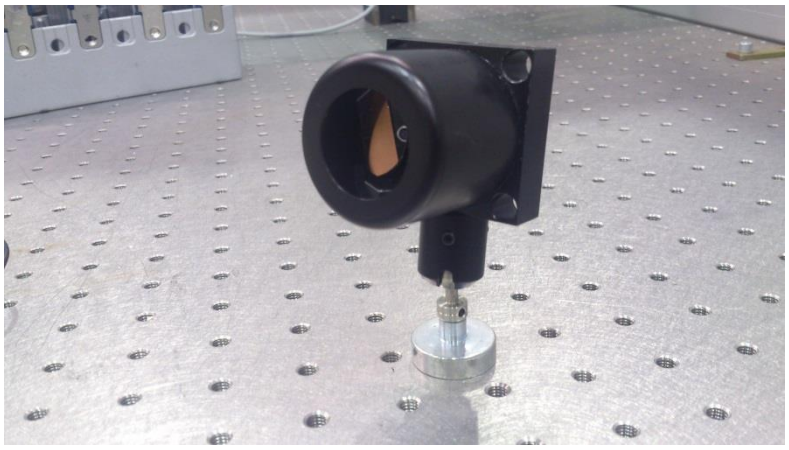

Figure 24 - Hollow retroreflector

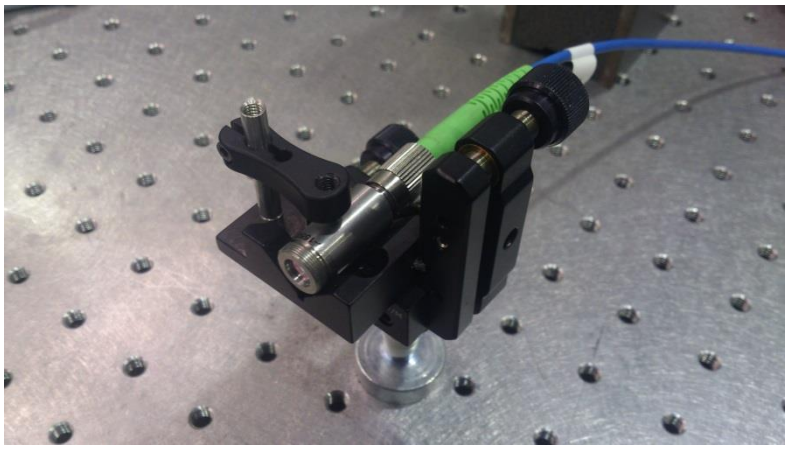

Figure 25 - Laser mounting and adjustment tool and collimator

4.2: The Position Sensitive Detector (PSD) THORLABS PDQ30C

The PDQ30C is a large area, four quadrant type position sensing detector fitted with an Indium-Gallium-Arsenide (InGaAs) photodiode for precise path alignment of light in the 1000 to 1700 nm infrared (IR) range. The sensor is segmented into four separate active areas, allowing it to measure beams with a spot size up to 3 mm. For optimal use, a spot size diameter of less than 0.5 mm is recommended.

The sensor outputs three analog voltages. The X-axis and Y-axis signals are proportional to the light difference sensed by the left-minus-right and top-minus-bottom pairs of photodiode elements in the detector array, while the SUM signal is proportional to the total amount of light falling on the sensor. For more information consult the datasheet in [20]

Figure 26 shows the diagram of the PSD electric signals:

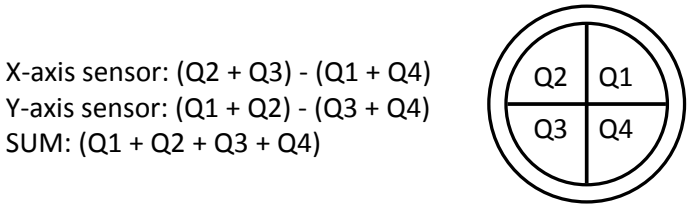

Figure 26 - PSD electric signals diagram

The segmented-quadrant position sensors consists of four distinct yet identical quadrant-shaped photodiodes that are separated by a ~0.1 mm gap and together form a circular detection area capable of providing a 2D measurement of the position of an incident beam. When light is incident on the sensor, a photocurrent is detected by each sector (labeled A, B, C, and D as shown in the Figure 27). From these signals difference signals can be determined using an appropriate A/D converter. The sum of all four signals is also determined for normalization purposes. The normalized coordinates (X, Y) for the beam's location are given by the following equations:

$$X = \frac{(A + C) - (B + D)}{A + B + C + D} = \frac{X_{Diff}}{SUM}$$

$$Y = \frac{(A + B) - (C + D)}{A + B + C + D} = \frac{Y_{Diff}}{SUM}$$

If a symmetrical beam is centered on the sensor, four equal photocurrents will be detected, resulting in null difference signals, and hence, the normalized coordinates will be (X, Y) = (0, 0). The photocurrents will change if the beam moves off center, thereby giving rise to difference signals that are directly proportional to the beam displacement from the center of the sensor. [21]

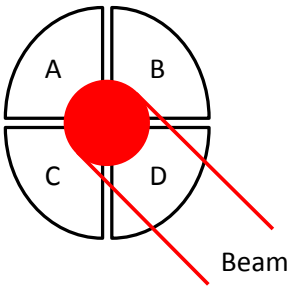

Figure 27 - PSD with an incident beam

Figure 27 presents an example of a incident laser beam in the PSD quadrant detector, while Figure 28 presents the Spectral Response of the PSD and Figure 29 shows a picture of the sensor.

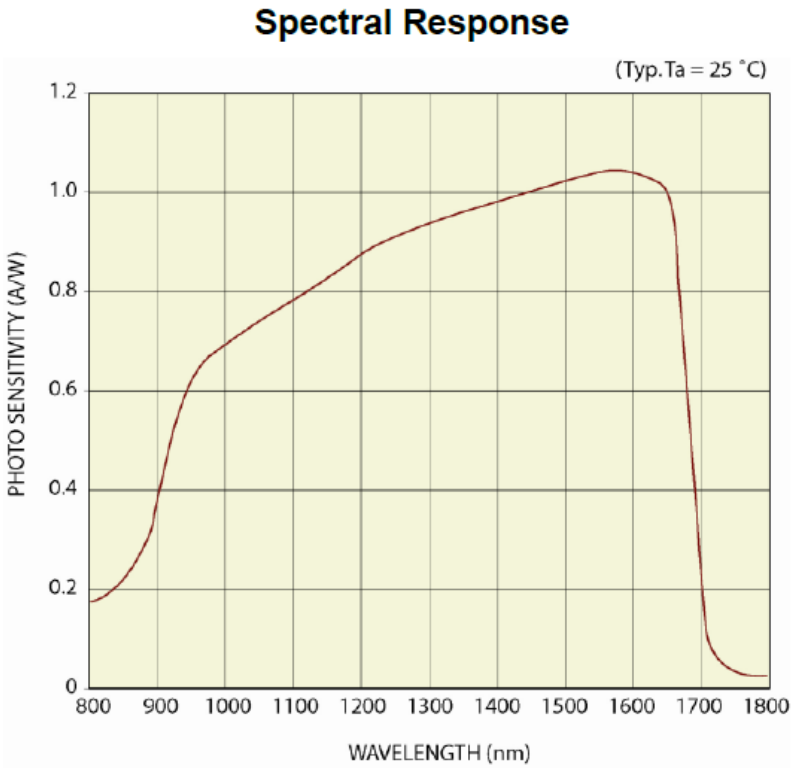

Figure 28 - PSD Spectral Response

Figure 29 - Position Sensitive Detector PDQ30C by THORLABS

4.2.1: Position Sensitive Detector (PSD) Technical Data

Electrical Specification

Wavelength Range 1000 – 1700 nm

Peak Responsivity 1 A/W @ 1630 nm

Transimpedance gain 10,000 V/A

Max Photocurrent 1 mA

Output Voltage Range ±4 V to ±14 V

Signal Output Offset 0.4 mV_{typ} (7 mV_{max})

Bandwidth 150 kHz

Recommended Spot size < Ø0.5 mm

Supply Voltage Requirement ±5V to ±15V DC, 35 mA

Operating Temperature 10 °C – 40 °C

Sensor Size Ø3.0mm

4.2.2: PSD Data Acquisition System

The TQD001 is a T-Cube Interface for use with the PDQ30C position sensing detector. Its top overlay has a 9-light display that indicates a beam's position on the sensor. The unit has three SMA connections for monitoring the X and Y difference signals as well as the sum signal. The T-Cube can also interface with a computer via USB1.1 and uses our APT software.

X & Y Diff Outputs Female SMA -10 V to >10 V

Sum Output Female SMA 0 to >10 V

X & Y Position Demand Outputs SMA 0 to >10 V

Closed Loop X & Y Position Control PID

Closed Loop Bandwidth 200Hz

USB Version 1.1

Input Voltage Requirements +15 V (200 mA), -15 V (50 mA), +5 V (50 mA)

Figure 30 - PSD data acquisition system

For more information consult the datasheet in [22]. The DAQ is shown in Figure 30.

4.3: The Cube Beamsplitter Edmund Optics

The model used was a Non-Polarizing Cube Beamsplitter 25mm 1100-1600nm (reference code: #47-236). For more information consult the datasheet in [23].

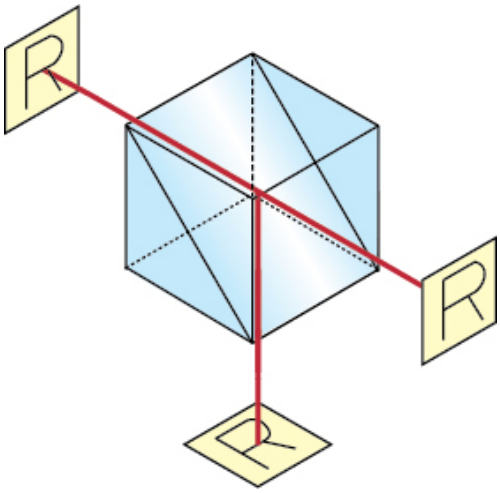

Figure 31 - Beamspliiter modus operandi

Figure 31 gives a basic idea of how the beamsplitter works and Figure 32 is a chart that relates the transmission rate with the laser beam wavelength, which for this case is 1550 nm.

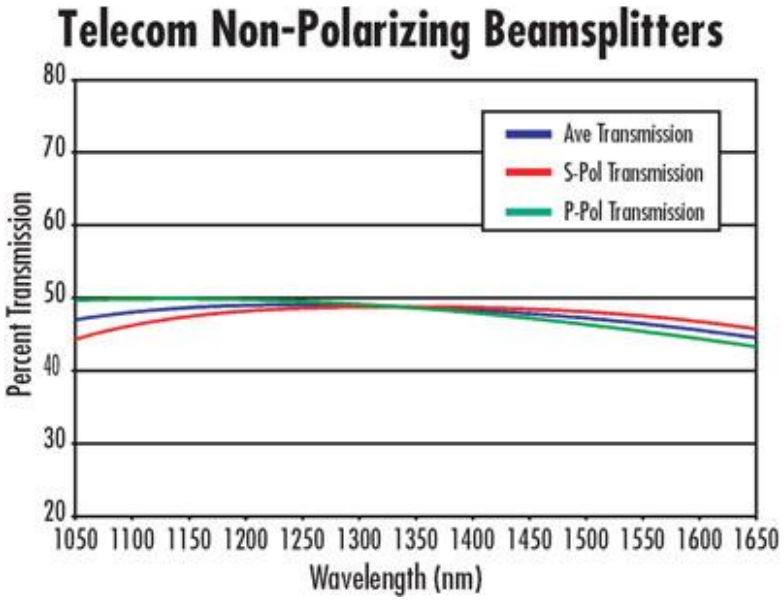

Figure 32 - Beamsplitter Chart Transmission versus Wavelenght

4.3.1: Beamsplitter Technical Data

Dimensions 25 mm

Dimensional Tolerance ±0.1 mm

Clear Aperture > 90%

Surface Accuracy (λ) 1/8

Surface Quality 40-20

Beam Deviation (arcminutes) ±2

Substrate N-BK7

Transmission 45 %

Transmission Tolerance ±5%

Absorption < 10%

Polarization < 6%

Coating Telecom: < 0.5% 1100 - 1620nm

4.4: Software Programming Language

4.4.1: The NI LABview Programming Language

National Instruments LABview was chosen because the student has a big knowledge of this programming language and there is a library developed by the PSD manufacturer (THORLABS) to read the data from the PSD data acquisition system.

LABview is a graphic programming language developed by National Instruments that provides fast development and virtual instrumentation as its biggest benefit.

4.4.2: The THORLABS Support Library

THORLABS provides a test software called “APT User” to test the sensor and perform some basic tasks. The library provided takes advantage of the “ActiveX” technology that can be implemented in LABview.

Chapter 5: Implementation of the Measurement System

5.1: PSD Calibration Development

The PSD amplitude output depends on the laser used, the laser shape and power. A calibration of the PSD sensor was necessary and a conceptual idea of how to perform this calibration was developed.

5.1.1: The Calibration Idea

There is a Linear Stepper Motor (from Newport model UE34CC) with a powerful resolution of 2 micrometers available in our workplace. The main idea consists in fixing each component of the system except the PSD, which is plugged in the Stepper Motor axis. All components are held while the PSD can perform small user predefined steps. These steps must follow one direction and the initial point must be the lowest or highest point of the PSD range according to the movement direction. If the movement is to up, initial point is the highest in PSD range and the opposite if the movement direction goes down. This methodology is good because it evaluates the whole PSD range, including the center where the PSD is more linear.

The simplified flow chart of the calibration procedure is (Figure 33):

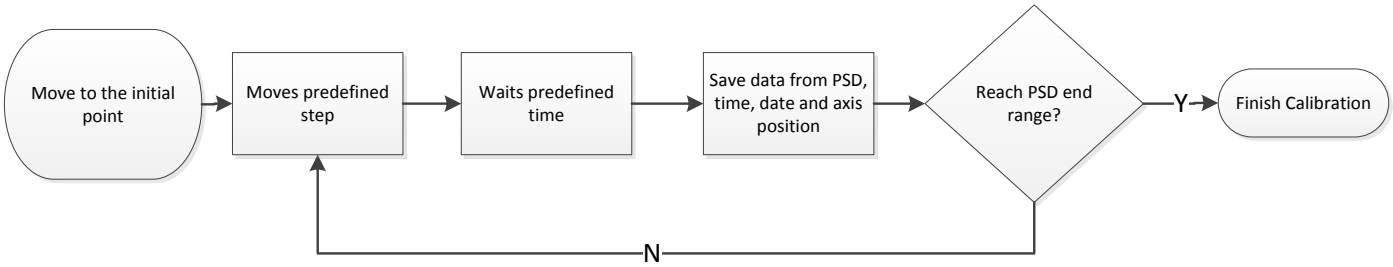

Figure 33 - Calibration flow chart

The results of this test return position data versus power intensity information from the PSD. Some linear fit can be performed on these results and returns how many volts per micrometer the PSD is able to develop for each axis (x and y).

Figure 34 shows a schema of the calibration setup.

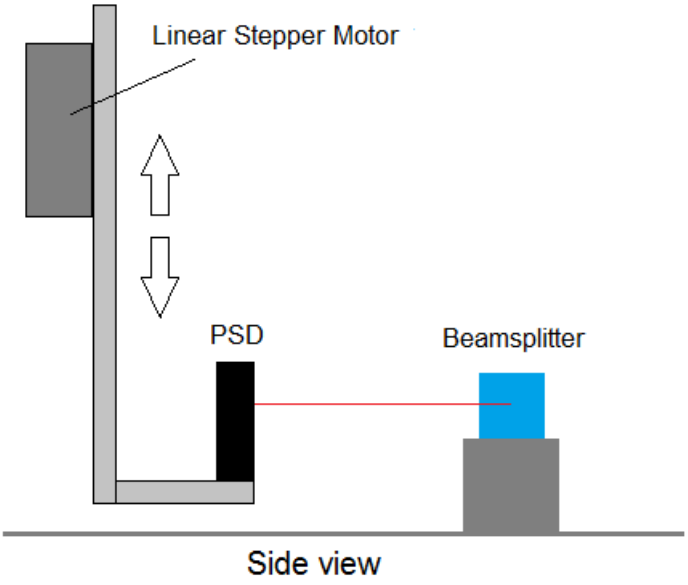

Figure 34 - Calibration schema

5.1.2: Calibration Software

The main functions of the calibration software are:

- Control the Newport stepper motor
- Acquire data from the PSD DAQ
- Show graphically the laser position in the PSD
- Control the calibration procedure
- Save the data from the calibration:
    - Position data from the stepper motor;
    - Xdiff, Ydiff e SUM signals from PSD;
    - Time and data from computer.

The software was developed in LABview programming language as described before.

The implementation of the control of the Newport Stepper Motor is made with the LABview library provided by Newport. The main functions in use are: Homing (moves to home position), Move Absolute, Move Relative, Set Parameters (speed and acceleration). The driver from Newport is connected to a computer USB port.

The communication with the PSD data acquisition hardware is made by USB. The software is able to read the data from the PSD: the Xdiff, Ydiff and SUM signals. The software uses a function from the PSD DAQ library that allows to show

graphically the laser position in the PSD, what was really helpful to perform the alignment for the calibration.

A flow chart of the calibration procedure was developed and implemented in the software. The flow chart of the calibration is shown in Figure 37.

During the calibration the program saves the data in a “TDMS” (Technical Data Management Streaming) file format. This is a LABview standard file format and it can be easily open in Microsoft Excel.

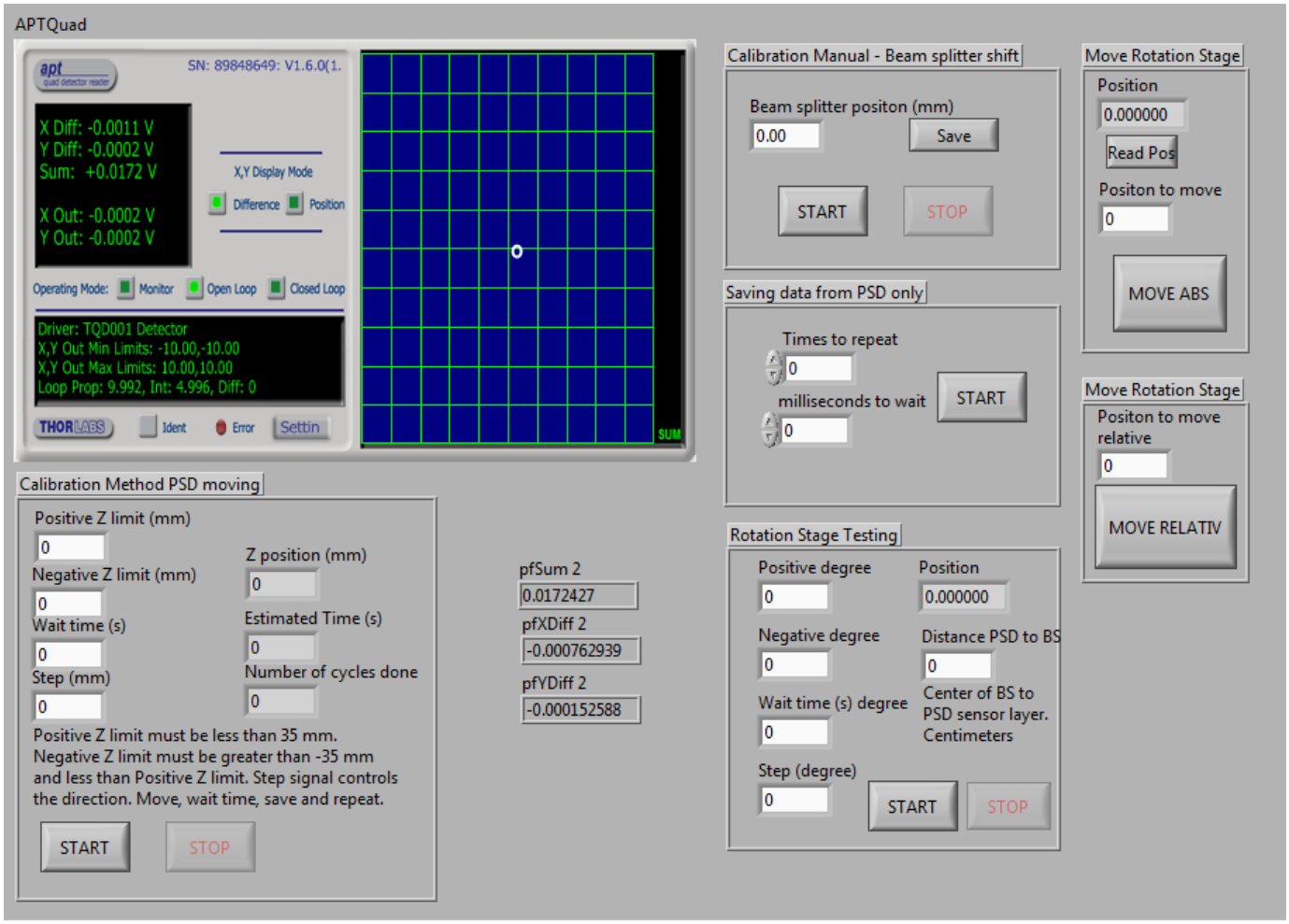

Figure 35 - Screenshot Calibration Software

Figure 35 shows a screenshot of the calibration software. The blue square with green lines shows the position of the laser beam dot in the PSD sensor. The box “Calibration Method PSD moving” is the user interface to control the calibration of the PSD. The range of the calibration is set using “Positive and Negative Z” (Z refers to the axis of the Linear Stepper Motor) limit and the other parameters are “Wait time” and “Step” size. The “Saving data from PSD only” saves data from the PSD

according to the “Times to repeat” and “milliseconds to wait”. This box pretends to get the background value from the ambient light and other perturbations that affect the measurement, for this test there is no laser beam in the sensor, just the sensor in stand-by mode.

The software includes functions for other forward tests. The “Rotation Stage Testing” works similarly to the “Calibration Method PSD moving”, but now the software control the rotation stage and not the Linear Stepper Motor anymore. This box is used for the Rotation Stage validation idea.

X volts	Y volts	Sum	Z position	Date	Time	X volts/sum
0,059357643	0,000762939	0,094758525	13,606	20.05.2014	17:57:54	0,62640953
0,059662819	0,000762939	0,095063709	13,612	20.05.2014	17:57:55	0,62760879
0,059662819	0,000762939	0,095216297	13,618	20.05.2014	17:57:56	0,62660302
0,059662819	0,000762939	0,09552148	13,624	20.05.2014	17:57:57	0,62460107
0,059662819	0,000762939	0,095368885	13,63	20.05.2014	17:57:57	0,62560047
0,059967995	0,000762939	0,09552148	13,636	20.05.2014	17:57:58	0,62779591
0,059967995	0,000762939	0,095674068	13,642	20.05.2014	17:57:59	0,62679466
0,059967995	0,000762939	0,095826656	13,648	20.05.2014	17:58:00	0,62579659
0,06027317	0,000762939	0,096131846	13,654	20.05.2014	17:58:01	0,62698443
0,06027317	0,000762939	0,096284434	13,66	20.05.2014	17:58:02	0,6259908
0,06027317	0,000762939	0,096437022	13,666	20.05.2014	17:58:03	0,62500033
0,06027317	0,000762939	0,096742205	13,672	20.05.2014	17:58:04	0,6230287
0,060578346	0,000762939	0,097352564	13,678	20.05.2014	17:58:04	0,62225732
0,060578346	0,000762939	0,09765774	13,684	20.05.2014	17:58:05	0,6203128
0,060578346	0,000457764	0,097962923	13,69	20.05.2014	17:58:06	0,61838034
0,060578346	0,000457764	0,098268099	13,696	20.05.2014	17:58:07	0,61645994
0,060883522	0,000762939	0,098573282	13,702	20.05.2014	17:58:08	0,6176473
0,060883522	0,000762939	0,099031046	13,708	20.05.2014	17:58:09	0,61479227
0,060883522	0,000457764	0,098878458	13,714	20.05.2014	17:58:10	0,61574101
0,060883522	0,000457764	0,099336237	13,72	20.05.2014	17:58:11	0,61290345
0,060883522	0,000457764	0,099641412	13,726	20.05.2014	17:58:12	0,61102628
0,060883522	0,000762939	0,099946596	13,732	20.05.2014	17:58:12	0,60916054
0,060883522	0,000762939	0,100251772	13,738	20.05.2014	17:58:13	0,6073062
0,061188698	0,000457764	0,100556955	13,744	20.05.2014	17:58:14	0,60849792
0,061188698	0,000762939	0,100862131	13,75	20.05.2014	17:58:15	0,6066568
0,061188698	0,000457764	0,101014733	13,756	20.05.2014	17:58:16	0,60574033
0,061188698	0,000457764	0,101319909	13,762	20.05.2014	17:58:17	0,60391584
0,061188698	0,000457764	0,101625092	13,768	20.05.2014	17:58:18	0,60210226
0,061188698	0,000457764	0,101930268	13,774	20.05.2014	17:58:19	0,60029959
0,061188698	0,000457764	0,102235451	13,78	20.05.2014	17:58:20	0,59850763

Figure 36 - Example data from calibration

Figure 36 - Example data from calibration shows how the data from the calibration is saved. There is one column to Xdiff (X volts), one to Ydiff (Y volts), SUM, Z position (Linear Stepper Motor position), Date and Time and for this measurement (X axis) X axis signal normalized (X volts/Sum).

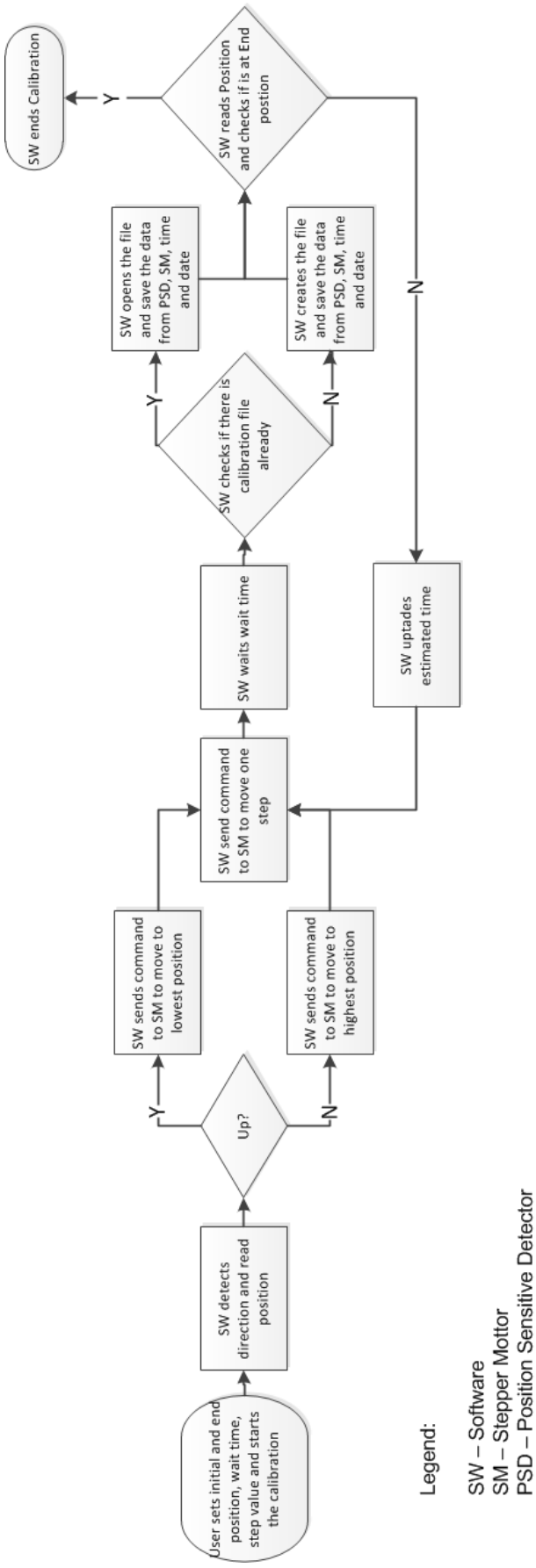

Figure 37 - Calibration software flow chart

5.2: Mount for the Complete System

A mount for the system was developed. In this mount the 2 PSDs, the beamsplitter and the retroreflector are able to fit. Figure 38 shows the CAD file for the mount. The bigger hole in the front side is for the laser beam go throw. The beamsplitter is transparent while the PSDs and the retroflector are black. There is a cover that closes the mount on purpose to be dark inside and reduce perturbations in the PSD sensor caused by the light.

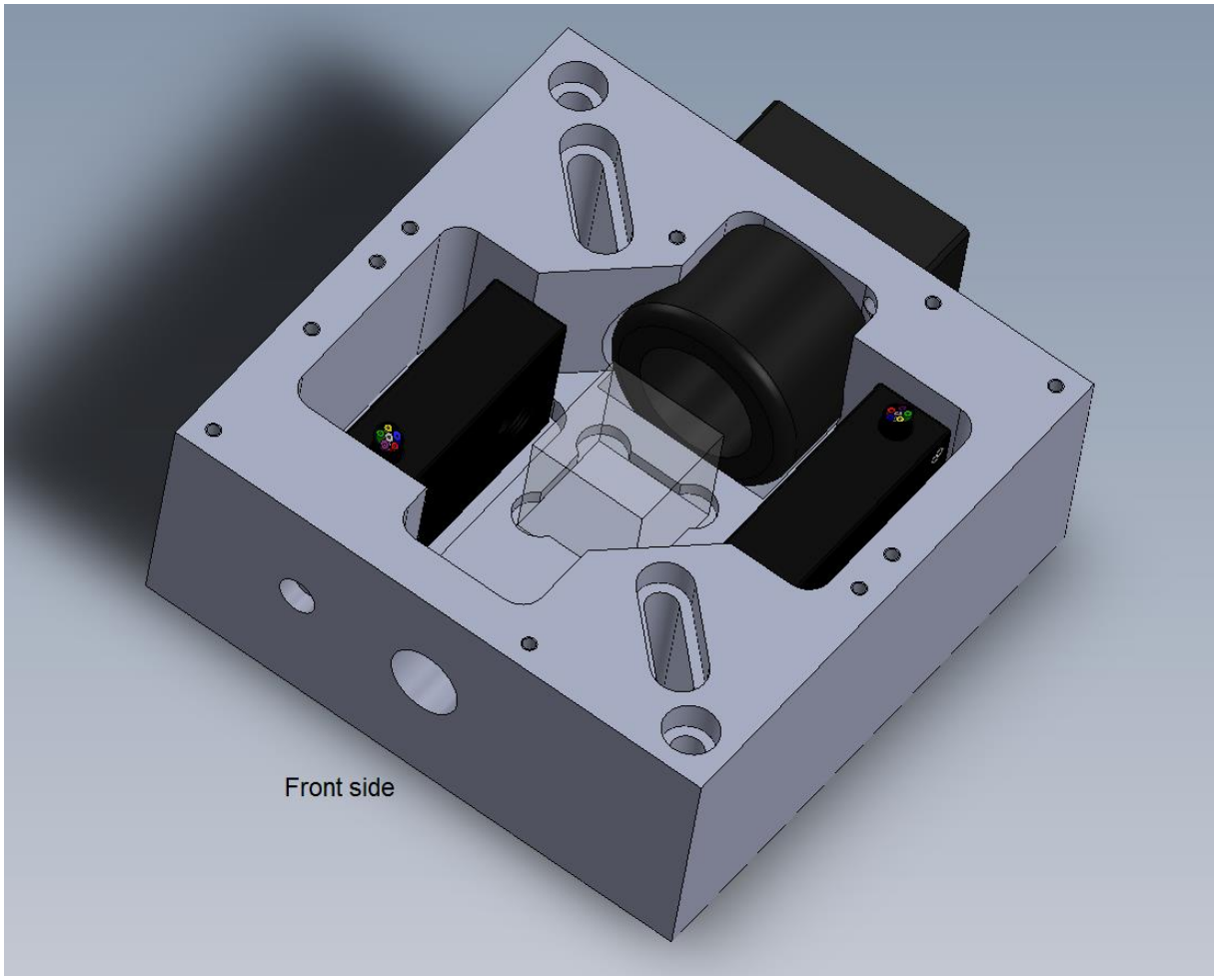

Figure 38 - Screenshot from the Mount CAD File

5.3: Validation Ideas for the Measurement System

After the calibration of the Position Sensitive Detector (PSD) the system is able to perform all the measurements required. The measurement system needs validation, for this purpose two ideas were analyzed on how to compare the measurements of the system with another reliable measurement system.

5.3.1: Rotation Stage Validation

The next set-up was done with a rotation stage machine. This rotation machine can be controlled by the computer. The idea consists in inserting the rotation stage into the system, fixing the beamsplitter in the center of the rotation stage and perform small rotation steps. The rotation position data from the rotation stage can be compared with the data from the PSD. This aims to test the rotation measurement capability of the system.

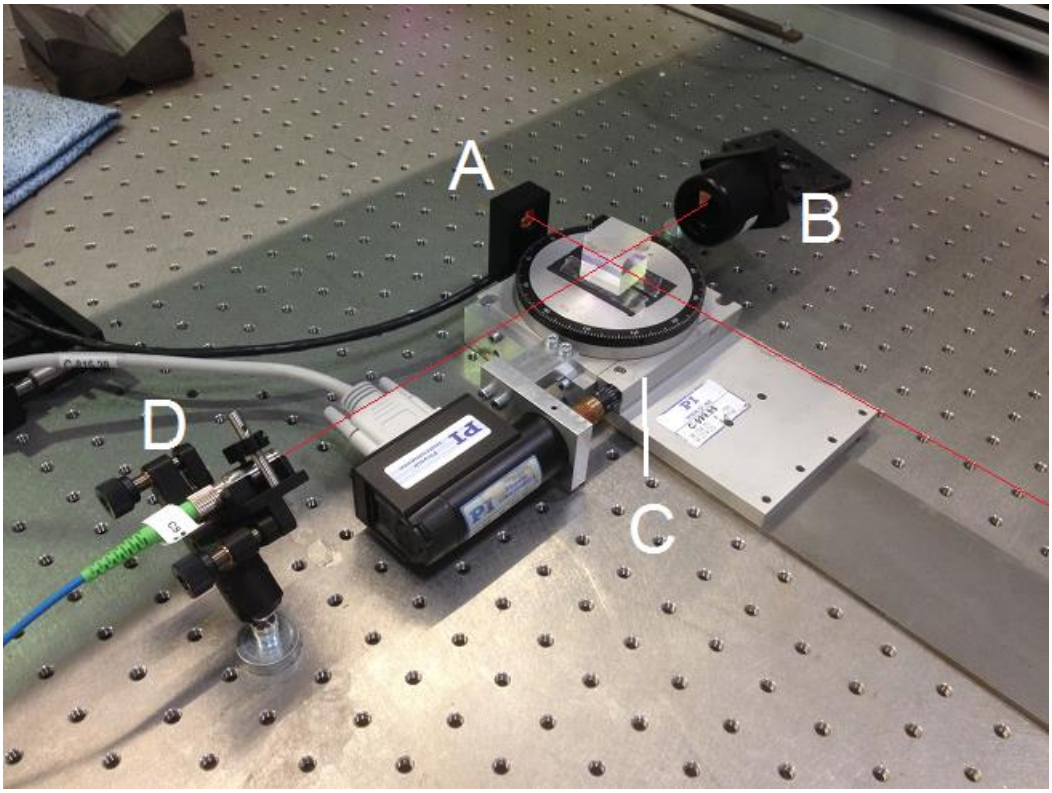

Figure 39 - Rotation Stage validation idea mount

The red laser beam in Figure 39 is illustrated to help the understanding, because the laser beam is invisible. The A letter represents the PSD, the B letter represents the retroreflector, the C letter represents the Rotation Stage Machine and the D letter represents the Laser Source (collimator).

5.3.2: Length Measurement Validation

The Absolute Multiline System is responsible for length measurement. The Multiline does not perform the same measurement as normal, because now there is the beamsplitter in the laser beam path. The influence of the beamsplitter must be

analyzed. For this, it can be performed for the same distance one measurement with the beamsplitter and another one without the beamsplitter in the laser beam path. The results of both measurements must be compared. If the beam splitter causes some difference in the result, a correction must be in the calculations of the length measurement. The same mounting of the rotation stage validation can be used, but the beamsplitter must be perpendicular to the laser source and not rotated.

Chapter 6: Results

6.1: PSD Calibration Results

The calibration procedure of the PSD presented interesting results and proved that is possible to use the sensor for the desired objective. All calibration measurements were done according to the procedure explained in section 5.1.1. Totally there were performed 10 measurements for each axis and then a weighted mean was applied. This aims to look for the repeatability of the sensor. After the weighted mean, a linear least square fit [24] was applied and the straightness of the each axis was analyzed. Theoretically, both axes should deliver the same calibration results, but some differences can happen due to the alignment, vibration, light and other perturbations.

The next charts (Figure 40 and Figure 41) show a calibration measurement for each axis. In the chart, the left upper chart shows the position in the PSD (Xdiff or Ydiff signal divided by the SUM signal versus) versus the position in the Linear Stepper Motor. The lower chart on the left shows the signal shift in the other axis (should be constantly zero but alignment errors cause some shift). The upper chart on the right shows how the residuals from the linear least square fit change, in the best straightness case it should stay constant. The lower right chart shows a zoom from the selected area of the lower left chart. The theory of the sensor asserts that the sensor is more linear in the center and this is seen clearly in the graph PSD position versus Linear Stepper Motor position, because the measurement is made from one border to the other border of the sensor. Based on this, the center area of the sensor is more linear and was chosen to be used, the red line area.

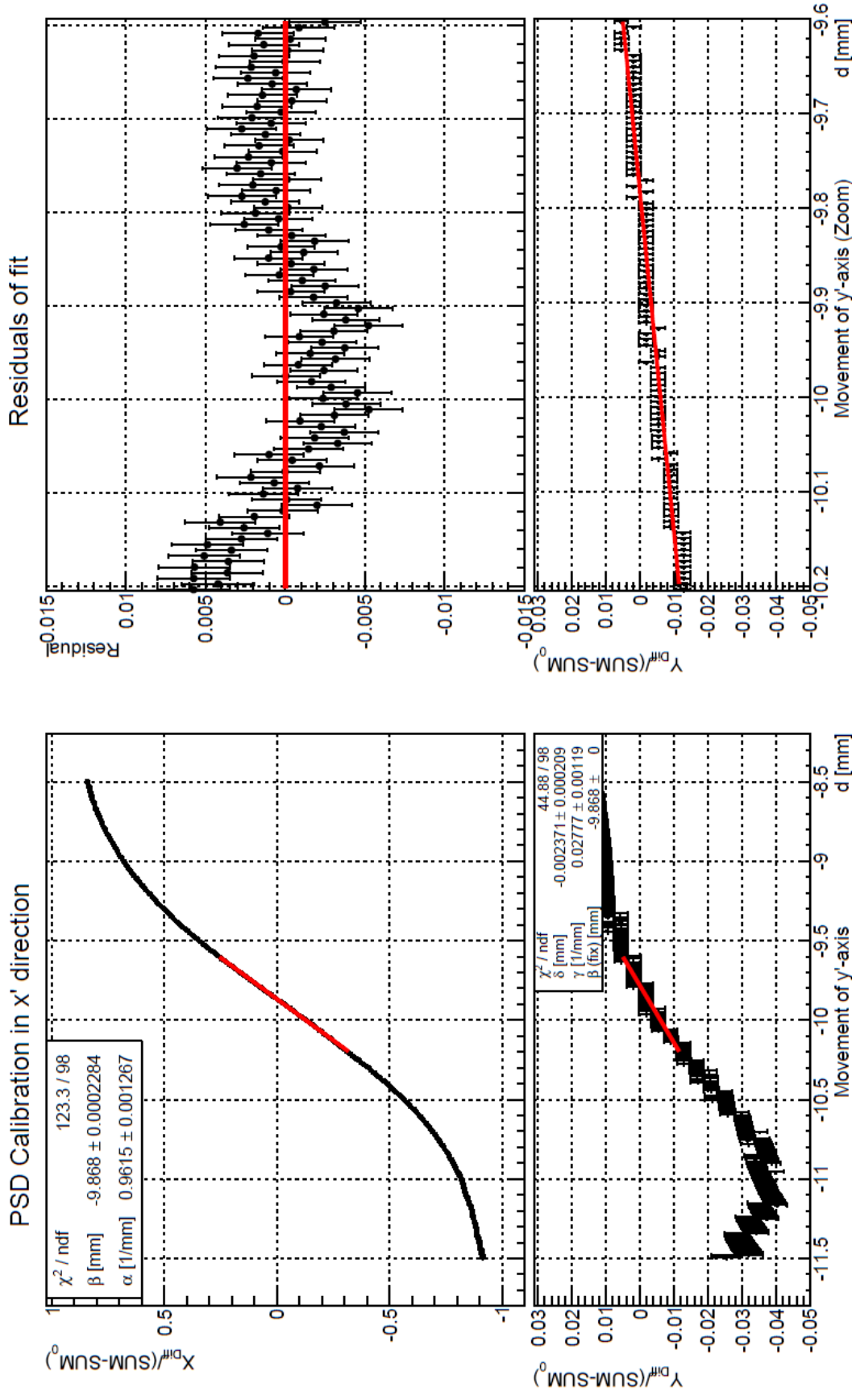

Figure 40 – Calibration chart from PSD X axis

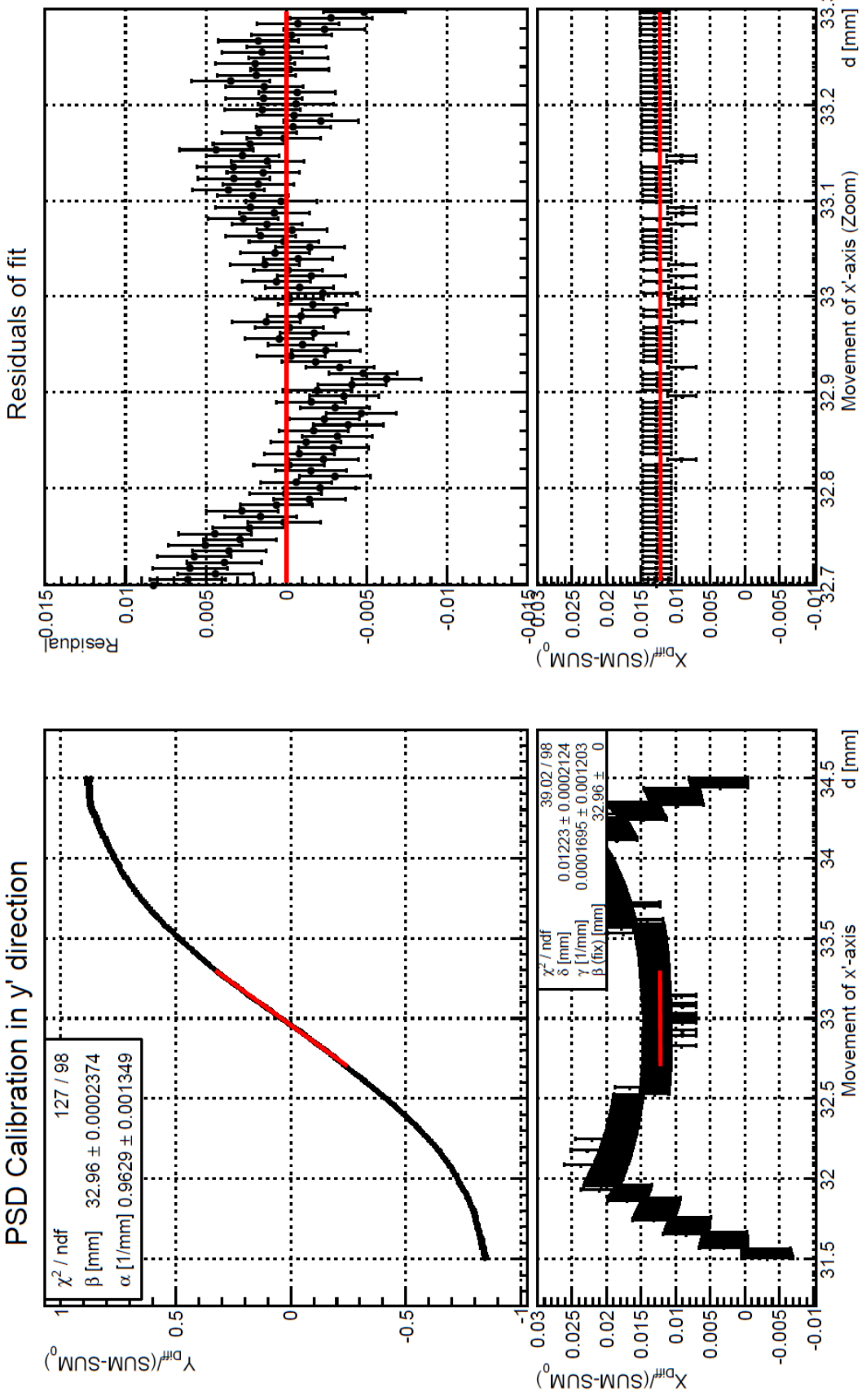

Figure 41 - Calibration chart from PSD Y axis

Due to the lack of repeatability of the system, setup not stable, difficult to perform the same alignment, beside others, a statistical weighted mean was applied.

From the statistical weighted mean:

$$\bar{x} = \frac{\sum_{i=1}^{n} x_i \cdot \sigma_i^{-2}}{\sum_{i=1}^{n} \sigma_i^{-2}}$$

$$\sigma_I = \sqrt{\frac{1}{\sum_{i=1}^{n} \sigma_i^2}} \qquad \sigma_O = \sqrt{\frac{1}{n-1} \frac{\sum_{i=1}^{n} (\bar{x} - x_i)^2 \cdot \sigma_i^{-2}}{\sum_{i=1}^{n} \sigma_i^{-2}}}$$

The results from the weighted mean for each axis are:

$$x': \quad \bar{x} = 0.9930 \frac{1}{\text{mm}} \quad \sigma_I = 0.0004 \frac{1}{\text{mm}} \quad \sigma_O = 0.0149 \frac{1}{\text{mm}}$$
$$y': \quad \bar{x} = 0.9831 \frac{1}{\text{mm}} \quad \sigma_I = 0.0004 \frac{1}{\text{mm}} \quad \sigma_O = 0.0064 \frac{1}{\text{mm}}$$

$$signal\ x' = p * \bar{\alpha}$$

$$signal\ y' = p * \bar{\alpha}$$

The "p" is the distance from the PSD center to the laser position in the PSD. The "σ" refers to inner error, the statistical error from the uncertainty of each individual error. The "σ_o" is the compatibility error and it is bigger due to the difficulty of reproducing equal measurements.

Beside the statistical errors from the weighted mean, we still have some fluctuation in the PSD signal value, this error is about 0.0004 volts. As SUM and Ydiff or Xdiff are used, this error is doubled. There is an association of errors and after some calculation, it returns the error is about 3%.

The accuracy of the sensor, in the best case, is 1 micron plus 1 micron for each 100 microns error. The results prove that the sensor has enough performance to be used for the expected objective.

The calibration presented some errors and had to be redone several times. Errors according to the ground vibration, luminosity and alignment of the laser beam mainly. The PSD showed to be very sensitive to touches in the fiber optic cable, so it is necessary to be careful with the fiber cables during measurements.

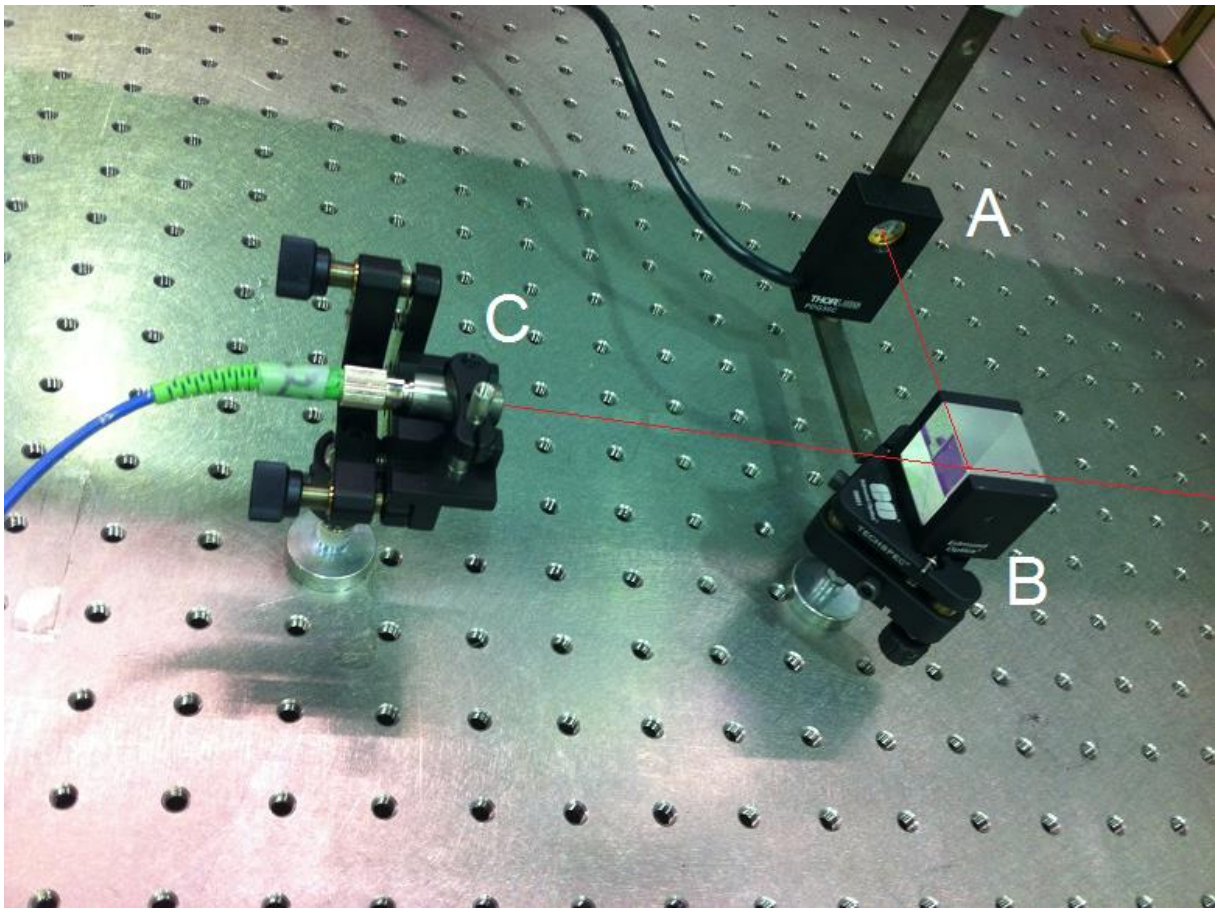

Figure 42 - Calibration of Y axis of the PSD

Figure 42 shows the mount for one calibration measurement for the Y axis. The PSD is fixed into the Linear Stepper Motor axis. The red laser beam is illustrated to help the understanding, because the laser beam is invisible. The A letter represents the PSD, the B letter represents the Beamsplitter and the C letter represents the Laser Source (collimator).

6.2: Validation Results

This section presents the results from the validation ideas presented in section 5.3.

6.2.1: Rotation Stage Results

The distance from the center of the beamsplitter to the center of the PSD sensor surface (“d”) was measured manually, but as mentioned before there is a big error associated with this measurement. The result was 82.00 ± 3.00 mm.

The PSD calibration software was adapted to control the rotation stage and save the data for this test. The software saved the angle position of the rotation stage, the Xdiff and SUM signals. A chart (Figure 43) was made based in the validation test results. The curve in the chart is position in the PSD (Xdiff/SUM) versus angle in the rotation stage.

Analyzing the chart is possible to see that there is a linear area (the red line area) for small angle range. The red line is the least square fit applied to check the straightness. The angle "ϕ" is the center of the linear area. The 10.92 is the sum of the squares of the vertical deviations from the least squares fit. The distance "d" was calculated using the angle of the rotation stage and the position of the laser in the PSD. It returns a value of 84.37 ± 0.49 mm.

A comparison of both "d" measurements:

- Manual: 82.0000 ± 3.0000 mm
- Software: 84.3700 ± 0.4891 mm

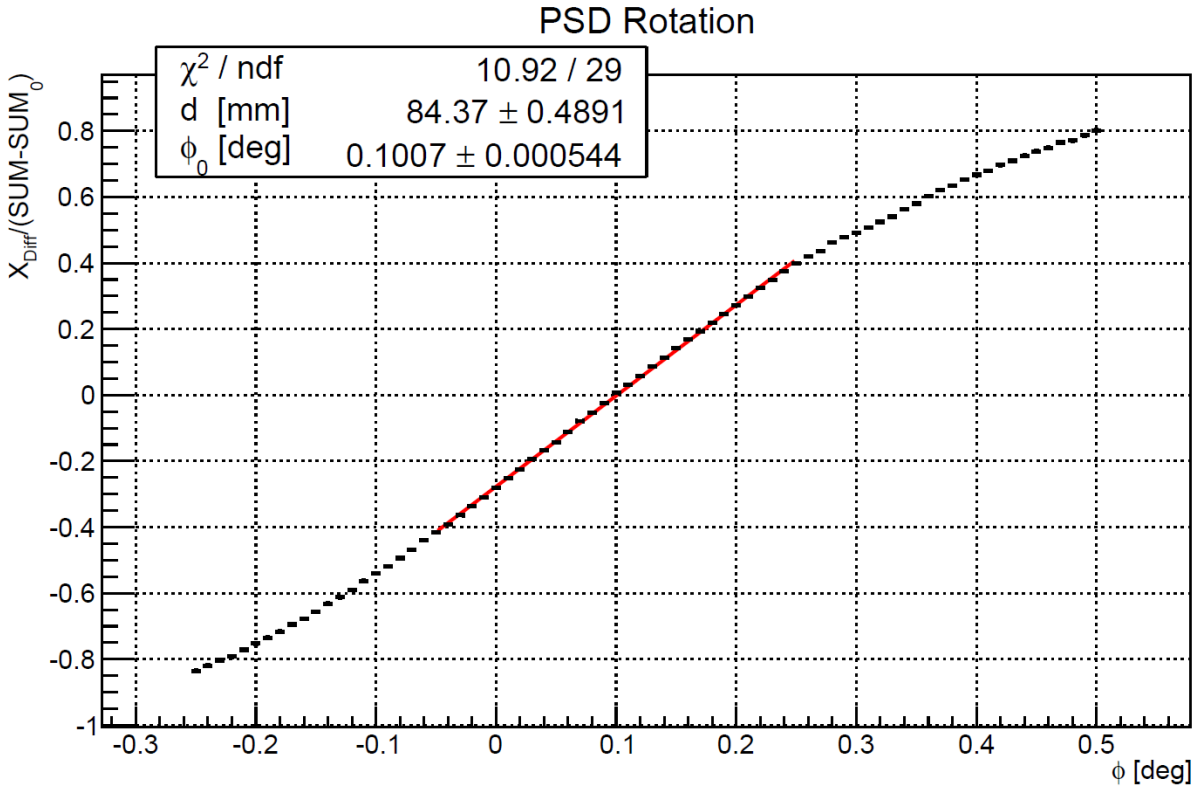

Figure 43 - Rotation measurement validation chart

There is a possible match of the results for "d" which proves that is possible to use the system to read the angle rotation. There is an acceptable error included due to the refraction in the beamsplitter that is not being taken into account. Further, a

best estimation for the manual measurement should be performed and a method to include in the calculation the refraction in the beamsplitter should be developed.

6.2.2: Length Measurement Results

The same length measurement was made in two different ways: one with the beamsplitter in the laser beam path and the other one without the beamsplitter in the laser beam path. It means that the laser source and the retroflector were kept in the same position for both measurements.

The measurements were performed by the Multiline System software, and were made 30 measurements for each method and the average was taken.

Results of the measurements:

Beamsplitter	**Measurement (mm)**
With	419.5887037
Without	406.5554768
Difference	13.0332269

The results show that the beamsplitter inserts some interference in the length measurement. The source of this error is because the Multiline System uses the index of refraction of the air for the whole laser beam path, but now there is some glass (25 mm) in the laser path two times because it is a round trip. The refraction index of the glass is bigger than the refraction index from the air. Basically the laser beam takes more time to develop the round-trip when the beam splitter is in the system and it makes Multiline System think the laser traveled a longer way.

A correction based on the results should be studied and implemented in the final software.

Chapter 7: Outlook

7.1: Conclusions

The results of the projects lead to conclude that is possible to use the concept of the proposed measurement system to measure the desired variables that are required to test the alignment of a machine tool. The measurement system can be used by itself to test the alignment or it can be integrated with another system in order to improve the performance and flexibility of the whole system.

The calibration procedure adopted to calibrate the Position Sensitive Detector (PSD) proved that the PSD develops a reliable performance and fits the accuracy requirements. The PSD can be used in another project with the knowledge based created by the project. The PSD was affected with a lot of small perturbations like ambient light, vibrations from other machines and the laser fiber cable not being stationary. All theses small effects were taken into account and helped to build a better mounting for the complete system. The Multiline alignment laser, that is visible, influenced in the PSD measurements, so there was a need of turning this laser off after aligning the laser and only keep the measurement lasers on to avoid noise.

The length measurement done by the Multiline System showed some differences from the normal length measurement, but corrections can be researched and applied to get the correct measurement values. This measurement can be performed even with the beamsplitter rotating small angles, just a correction need to be researched and developed. This procedure allows to have more than one different measurement at the same time, both rotation and length measurement can be performed in parallel.

The validation idea of the rotation measurement proved that the system delivers enough performance and fit the specifications for measuring small angles for machine tool alignment test.

Research and development still needs to be done to optimize the concept and test some improvements and variations that can be applied to the measurement concept. The final mount will turn the concept able to be used not only for alignment

of machine tool testing, but for any kind of machine that performs similar movements. All the results show that the measurement system has a great future.

7.2: Further Research Questions

The following steps of the project consist in developing the final software, based on the calibration software, in order to read out all the measurements and return the values to the user and produce the mounting for the system and mount and test the system in the new mounting. The second Position Sensitive Detector (PSD) must be bought and calibrated the same way as the first PSD to complete the measurement system. The second PSD will bring new possibilities for the system, like to read both PSDs at the same time to improve the result reliability.

The project showed other interesting topics of research like the influence of the glass of the beamsplitter in the interferometry measurement made by the Multiline System. This research can be applied to the system to help improve the performance.

The calculation of the rotation measurement does not take into account the diffraction and refraction that can occur when the incidence angle of the laser is different from zero degree (into the beamsplitter surface). A new calculation including the diffraction and refraction of the laser beam could be studied and developed. The results of both measurements could be compared and analyzed.

The measurement system developed is portable (the sensor mount) and maybe can be applied to other measurement needs as robot alignment tests and other machines with the same or similar movements measured by the system.

A comparison with other methods actually used or in development in the laboratory for testing the alignment of machine tool should be performed, to help identifying possible advantages and disadvantages of the measurement system developed.

Furthermore, other validation ideas should be developed to test the measurement system and compare with the actual results.

Bibliografy

[1] H. Schwenke, W. Knapp, H. Haitjema, A. Weckenmann, R. Schmitt, F. Delbressine, “Geometric error measurement and compensation of machines—An update”, CIRP Annals - Manufacturing Technology, 2007.

[2] McKeown PA, Loxham J (1973) Some Aspects of The Design of High Precision Measuring Machines. Annals of the CIRP 22(1).

[3] ANSI/ASME B5.54 (1991) Methods for Performance Evaluation of Computer Numerically Controlled Machining Centers.

[4] Hocken R (1980) Technology of Machine Tools, vol. 5. Lawrence Livermore National Laboratory, University of California.

[5] Spaan HAM (1995) Software Error Compensation of Machine Tools, PhD Thesis, Eindhoven University of Technology.

[6] Weekers WG (1996) Compensation for Dynamic Errrors of Coordinate Measuring Machines, PhD Thesis, Eindhoven University of Technology.

[7] Bryan JB (1981) A Simple Method for Testing Measuring Machines and Machine Tools. Parts I & II. Precision Engineering 4(2):61–69; Bryan JB (1981) A Simple Method for Testing Measuring Machines and Machine Tools. Precision Engineering 4(3):125–138.

[8] Donmez MA, Blomquist DS, Hocken RJ, Liu CR, Barash MM (1986) A General Methodology for Machine Tool Accurracy Enhancement by Error Compensation. Precision Engineering 8:187–196.

[9] Soons JA (1992) Modeling the Errors of Multi-Axis Machines, A General Methodology. Precision Engineering 14(1):5–10.

[10] Delbressine FLM (2005) Modelling Thermomechanical Behaviour of Multi-Axis Machine Tools. Precision Engineering 30(1):47–53.

[11] Gruber, R., Knapp, W., 1998, Temperatureinflu¨ sse auf die Werkzeugmaschinengenauigkeit (Temperature influence to machine tool accuracy), Werkstatt und Betrieb 131:11.

[12] Schellekens P, Rosielle N, Vermeulen H, Vermeulen M, Wetzels S, Pril W (1993) Design for Precision, Current Status and Trends. Annals of the CIRP 47(2):557–586.

[13] Perreira PH, Hocken RJ (2007) Characterization and Compensation of Dynamic Errors of a Scanning Coordinate Measuring Machine. Precision Engineering 31(1):22–32.

[14] P. Hariharan, “Basics of Interferometry”, Elsevier Inc., 2007.

[15] P. A. Coe, D. F. Howell and R. B. Nickerson, “Frequency scanning interferometry in ATLAS: remote, multiple, simultaneous and precise distance measurements in a hostile environment”. University of Oxford, 2004.

[16] C. Lu, Y.-S. Zhai, X.-J. Wang, Y.-Y. Guo, Y.-X. Du, G.-S. Yang.” A novel method to improve detecting sensitivity of quadrant detector” Elsevier Inc., 2014.

[17] T. Matsushita, S. Boogert, R. Devenish, and R. Walczak. “Optical alignment system for the ZEUS micro vertex detector”. Nucl. Instrum. Meth., A466:383-389, 2001.

[18] R. Bingham, E. Botcherby, P. Coe, G. Grzelak, A. Mitra, J. Prenting, A. Reichold. “The Linear Collider Alignment and Survey (LiCAS) Project”. LiCAS Group, Particle Physics sub-department, University of Oxford, UK, Applied Geodesy group, DESY, Germany,

[19] “Absolute Multiline Manual”. Etalon AG, 2013.

[20] “Product Specification Sheet Position Sensitive Detector PDQ30C”. THORLABS, 2010.

[21] Position Sensing Detectors. Thorlabs website. [Online] [Cited: June 30, 2014] http://www.thorlabs.com/newgrouppage9.cfm?objectgroup_id=4400

[22] “TQD001 Manual”. THORLABS, 2014.

[23] 25mm 1100-1600nm, Non-Polarizing Cube Beamsplitter. Edmund Optics website [Online] [Cited: June 30, 2014] http://www.edmundoptics.com/optics/beamsplitters/cube-beamsplitters/broadband-non-polarizing-cube-beamsplitters/47-236?&pModal=false&site=US&coun

[24] DALE, John. “A Study of Interferometric Distance Measurement Systems on a Prototype Rapid Tunnel Reference Surveyor and the Effects of Reference Network Errors at the International Linear Collider”, Oxford, 2009.